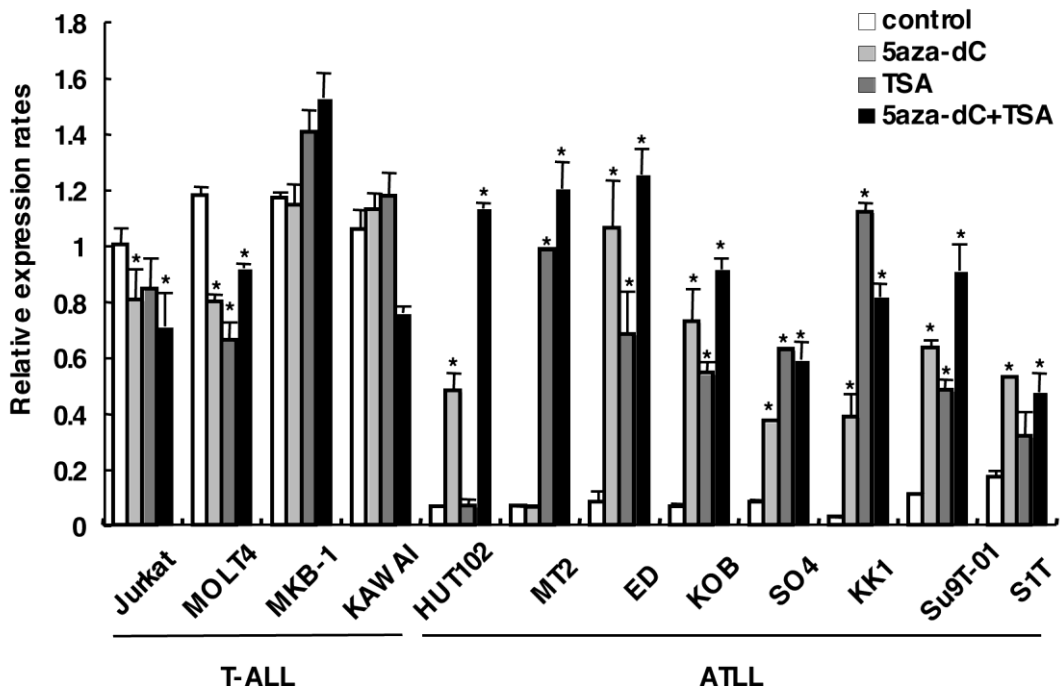

Supplementary Figure 1. An inhibitor of histone deacetylase, trichostatin A, and/or an inhibitor of DNA methylation, 5-aza-deoxycytidine, induces *NDRG2* expression in ATLL cell lines. Various T lymphoblastic leukaemia cell lines, including four T-ALL and eight ATLL cell lines, were cultured with 10 μM 5-aza-deoxycytidine (5-aza-dC) for 72 h (light gray bar), 1.2 μM trichostatin A (TSA) for 48 h (dark gray bar), or 1.2 μM of TSA for 48 h followed by 10 μM 5-aza-dC for 24 h (black bar). After the treatments, total RNA was extracted, and quantitative RT-PCR was performed with *NDRG2* and *β-actin*. The relative amounts of mRNA were normalized against *β-actin* mRNA and expressed relative to the mRNA abundance in the Jurkat cell line. The mean±s.d. is shown. *$P < 0.05$ compared with untreated control (Student's *t* test). The data are representative of two experiments.

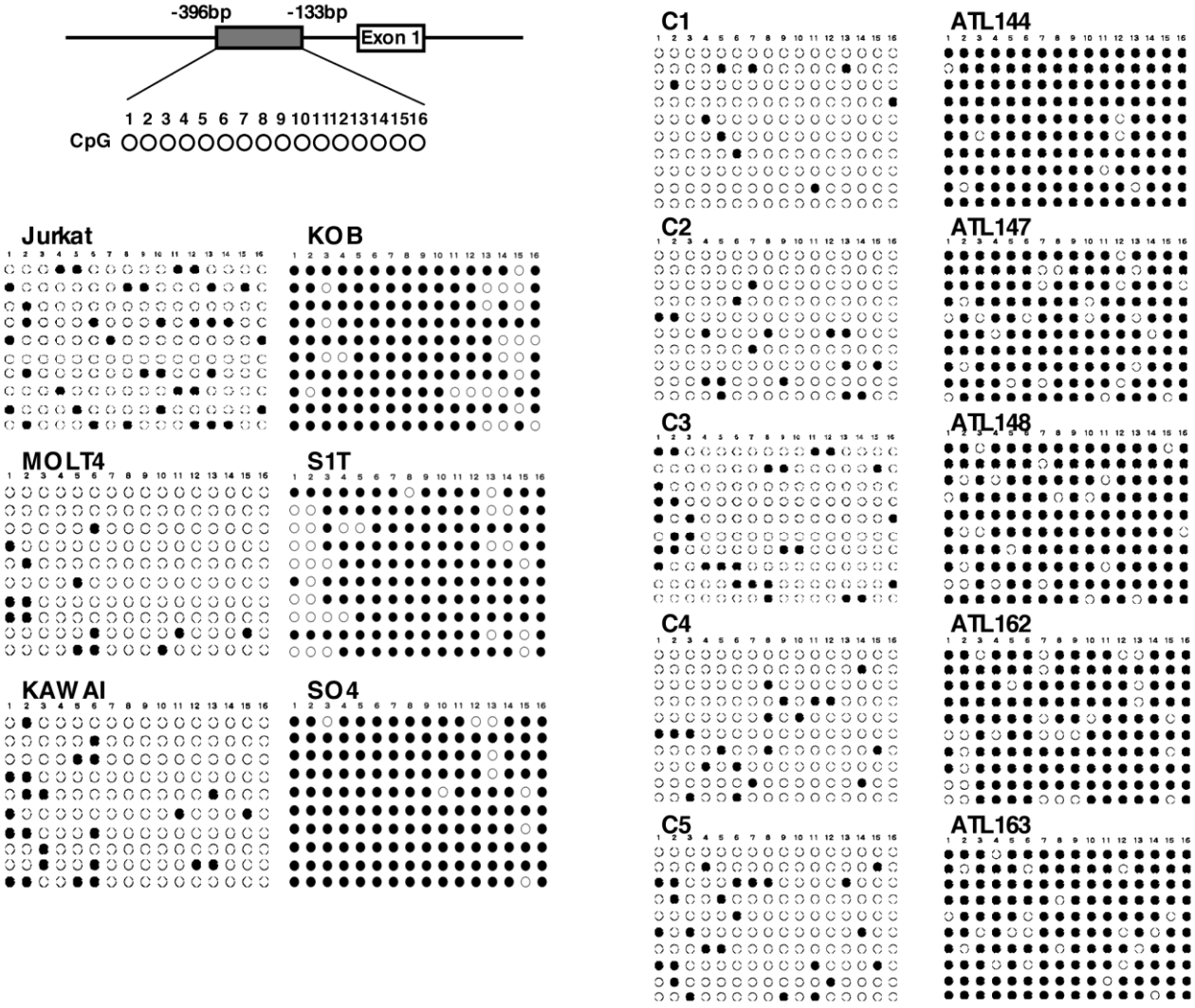

Supplementary Figure 2. Methylation of the *NDRG2* gene promoter in ATLL. Bisulfite genomic sequencing of the *NDRG2* promoter region in three T-ALL cell lines (Jurkat, MOLT4, and KAWAI), three ATLL cell lines (KOB, S1T, and SO4), and five samples each of $CD4^+$ T lymphocytes from normal volunteers (C1-C5) and of ATLL cells from patients (ATL144, ATL147, ATL148, ATL162, and ATL163). PCR products amplified from bisulfite-treated genomic DNA were subcloned, and 10 clones in each cell line were sequenced. Open circles indicate unmethylated CpGs (Thy), and filled circles indicate methylated CpGs (Cyt). The region sequenced spans from -396 bp to -133 bp and contains 16 CpGs sites.

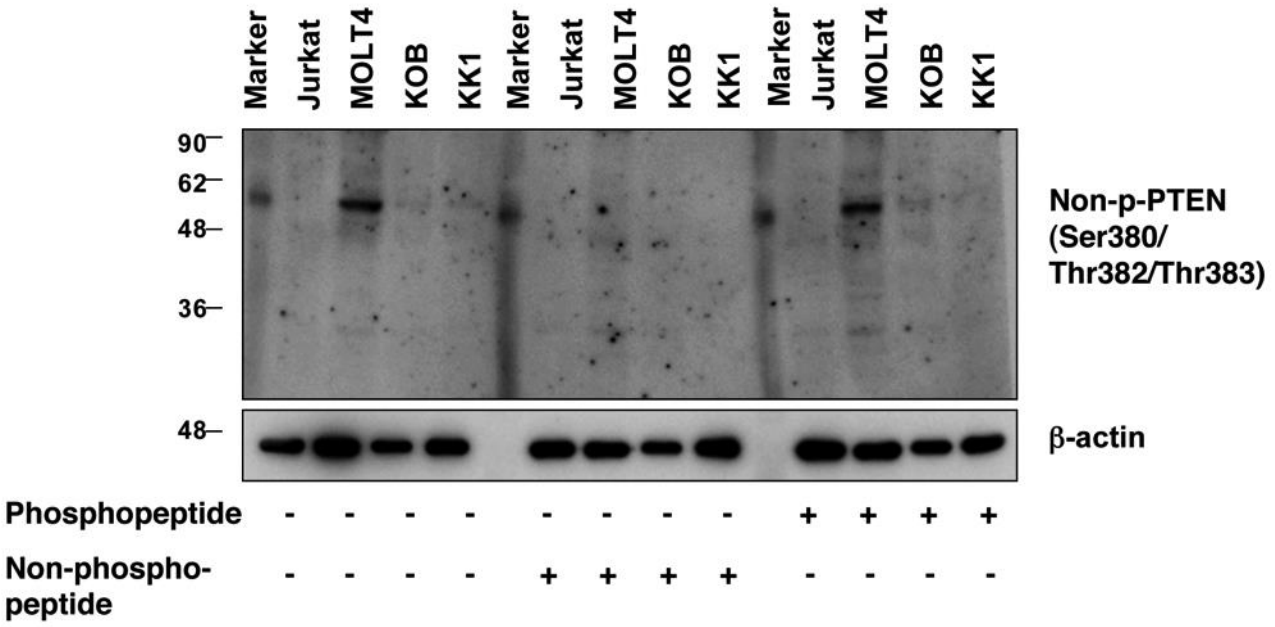

Supplementary Figure 3. Specificity of the non-phospho-PTEN antibody by peptide competition. Cell lysates were blotted and incubated with an antibody against non-phosphorylated PTEN (Ser380/Thr382/Thr383) (Cell Signaling Technology) at 1:1000 in the presence of 333 nM of phosphopeptide specific to phosphorylated PTEN (Ser380/Thr382/Thr383) (aa 373-390) or the corresponding non-phosphorylated peptide and in the absence of any blocking peptide. The specific band for the non-phosphorylated PTEN (Ser380/Thr382/Thr383) disappeared in the presence of the PTEN-non-phosphopeptide, but not the PTEN-phosphopeptide. The data are representative of two experiments.

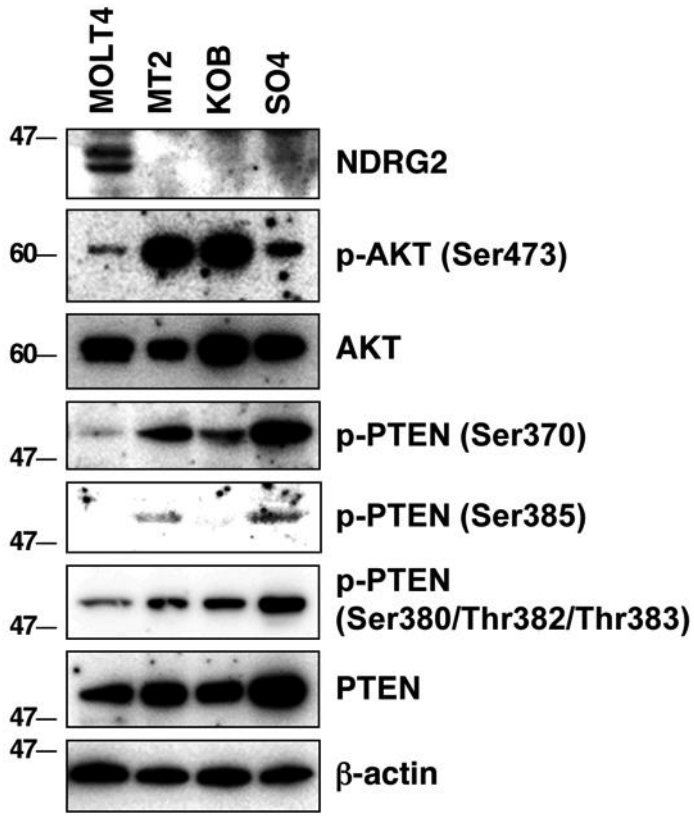

Supplementary Figure 4. An ATLL cell line, SO4, expresses higher levels of total and phosphorylated forms of PTEN. Western blot analysis of NDRG2, PTEN, p-PTEN (Ser370, Ser380/Thr382/Thr383, and Ser385), AKT, and p-AKT (Ser473) was performed in the T-ALL cell line MOLT4 and in three ATLL cell lines (MT2, KOB, and SO4). The data are representative of three experiments.

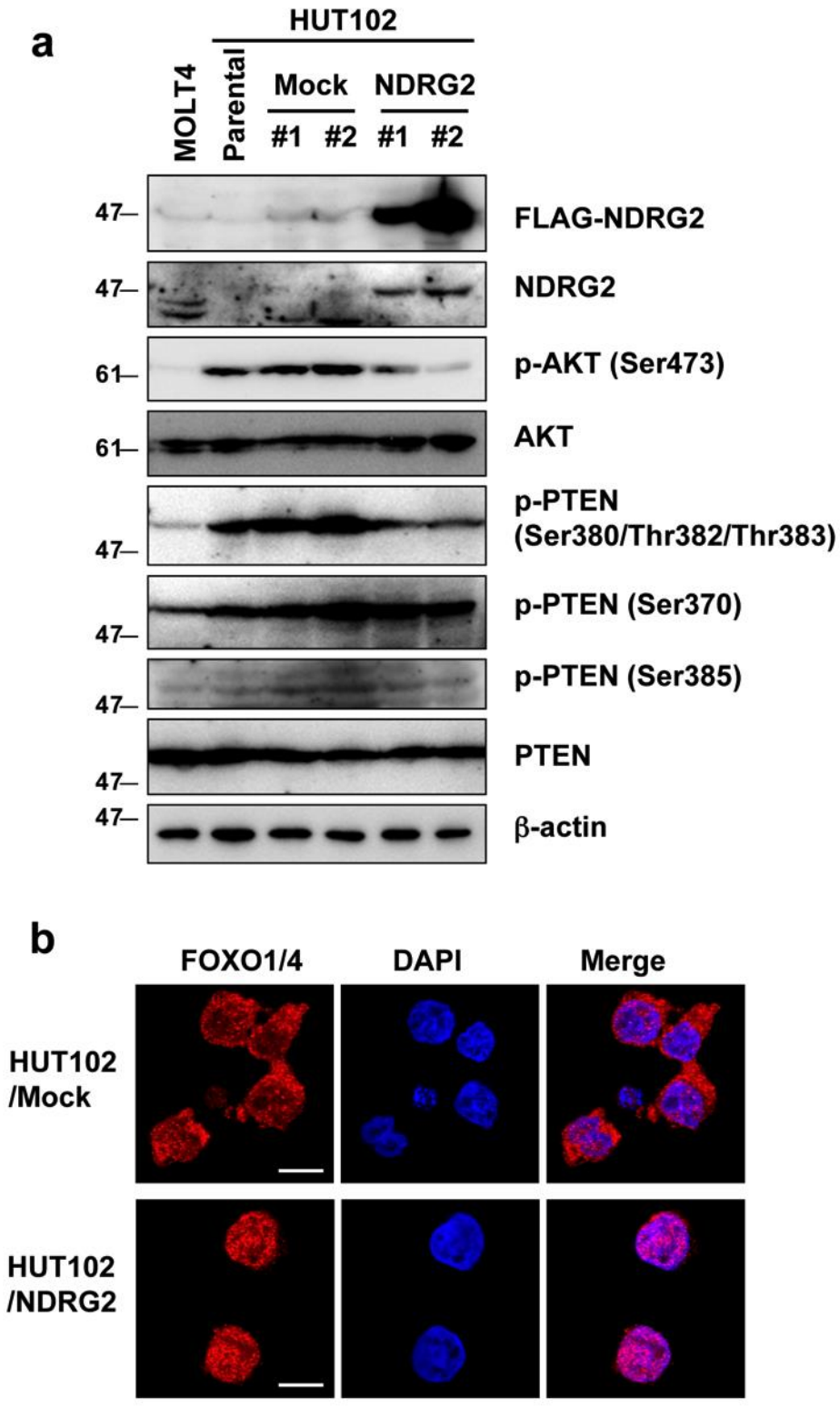

Supplementary Figure 5. Ectopic expression of NDRG2 induces dephosphorylation of PTEN at Ser380/Thr382/Thr383 and suppresses AKT activation in the ATLL cell line. (**a**) HUT102 cells were stably transfected with pCMV26 (Mock) or FLAG-NDRG2 expression vector and

analysed for protein levels of NDRG2, total PTEN, phosphorylated PTEN (Ser370, Ser380/Thr382/Thr383 cluster, and Ser385), total AKT, and phosphorylated AKT (Ser473). The data are representative of three experiments. (**b**) The localisation of FOXO1/4 in the mock- and NDRG2-transfected cells was determined by immunofluorescence using an anti-FOXO1/4 antibody (red). The nuclei were stained with DAPI (blue). Scale bar, 10 μm. The data are representative of three experiments.

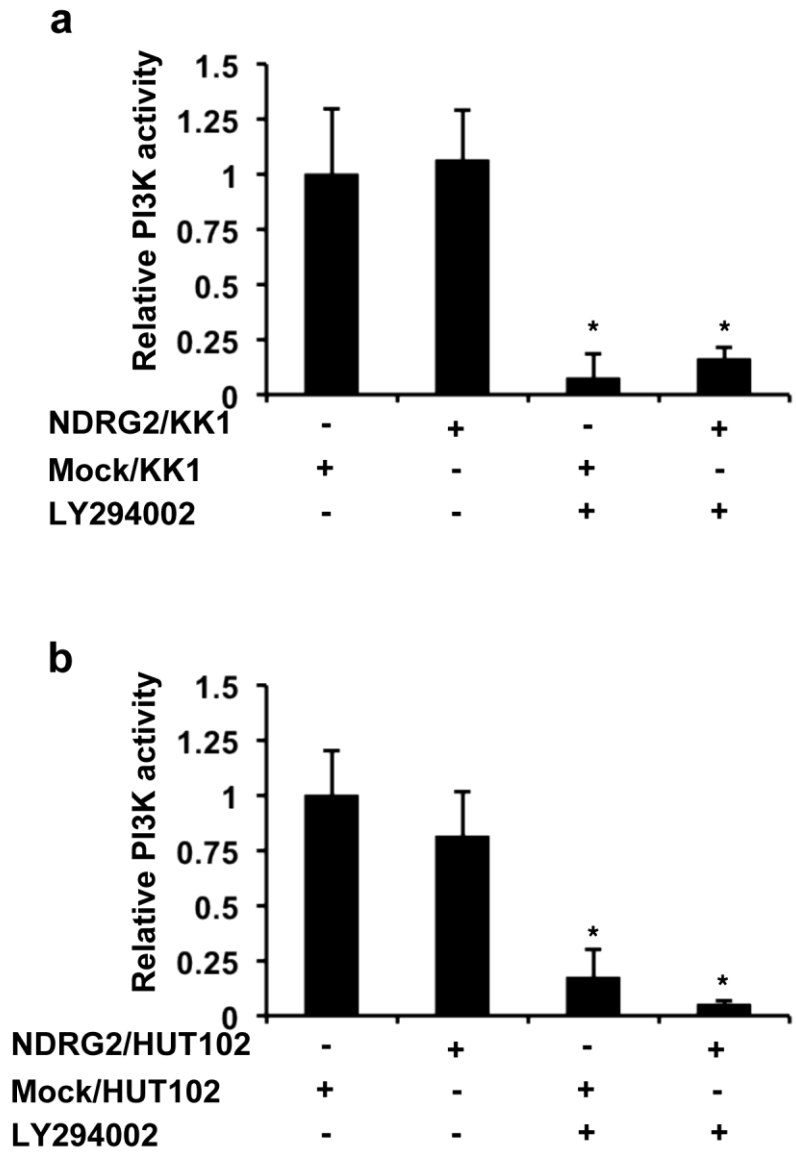

Supplementary Figure 6. NDRG2 expression in ATLL cell lines did not affect the basal activity of PI3K. Cell lysates from KK1 (a) or HUT102 (b) cells stably transfected with pCMV26 (Mock) or FLAG-NDRG2 expression vector were immunoprecipitated with an anti-p85 antibody and incubated with PIP_2 substrate in the presence or absence of 100 μM of the PI3K inhibitor LY294002. The amount of PIP_3 formed from PIP_2 by PI3K activity was detected using a competitive ELISA. Data are expressed relative to activity in the Mock-transfected control cells. The mean±s.d. is shown, $*P < 0.05$ (Student's *t* test). The addition of LY294002 in the reaction

mixture caused a significant decrease in kinase activity. The data are representative of two experiments.

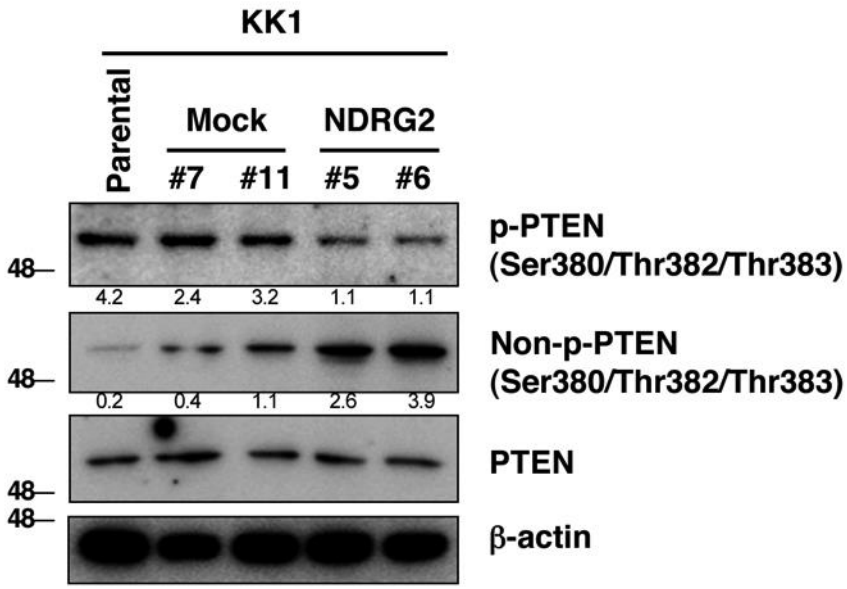

Supplementary Figure 7. Ectopic expression of NDRG2 increases the abundance of Ser380/Thr382/Thr383 non-phosphorylated PTEN in ATLL cell line. KK1 cells stably transfected with pCMV26 (Mock) or FLAG-NDRG2 expression vector were analysed for protein levels of total PTEN, phosphorylated PTEN (Ser380/Thr382/Thr383), and non-phosphorylated PTEN (Ser380/Thr382/Thr383). The value is the ratio of the band density of phosphorylated PTEN or non-phosphorylated PTEN divided by the band density of the corresponding total PTEN. The data are representative of three experiments.

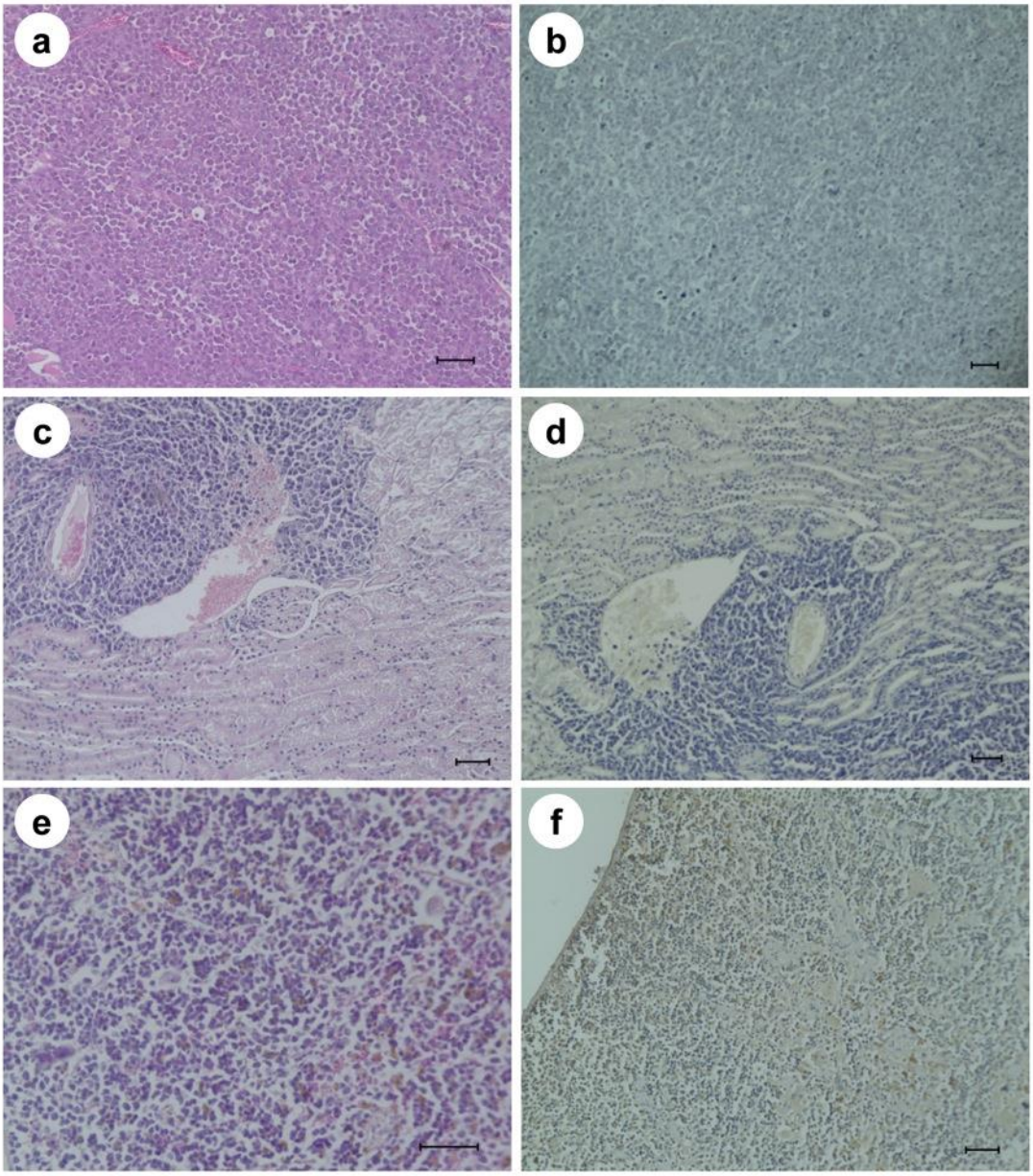

Supplementary Figure 8. Histopathological analyses of NOG mice injected intravenously with KK1-Mock or KK1-NDRG2 cells. Histological examination revealed lymphoma development as well as tumour cell infiltration in multiple organs in KK1-Mock-injected mice; however, KK1-NDRG2-injected mice only showed organ infiltration without lymphadenopathy. Representative histological images of each group are shown. Lymphoma sections from the mesenteric lymph node of a KK1-Mock-injected NOG mouse were subjected to histopathology (a,b). The results indicated

that monomorphic lymphoid cells were diffusely arranged into solid sheets. The tumour cells had scant cytoplasm with large round vesicular nuclei, and numerous mitotic figures were present. Kidney sections from a KK1-Mock-injected NOG mouse were examined by histopathology (c,d). The results demonstrated massive infiltration of pleomorphic lymphoid cells into the renal interstitial area. Spleen sections from a KK1-NDRG2-injected NOG mouse (e,f). The histopathology indicated the presence of a mixed population of mature lymphocytes and neoplastic lymphoid cells. The neoplastic cells (marginal area) demonstrated predominantly cytoplasmic immunopositive staining for FLAG-NDRG2 (f). All populations of neoplastic lymphoid cells from KK1-Mock-injected NOG mice were negative for the anti-FLAG antibody staining (b, d). Scale bar, 50 μm.

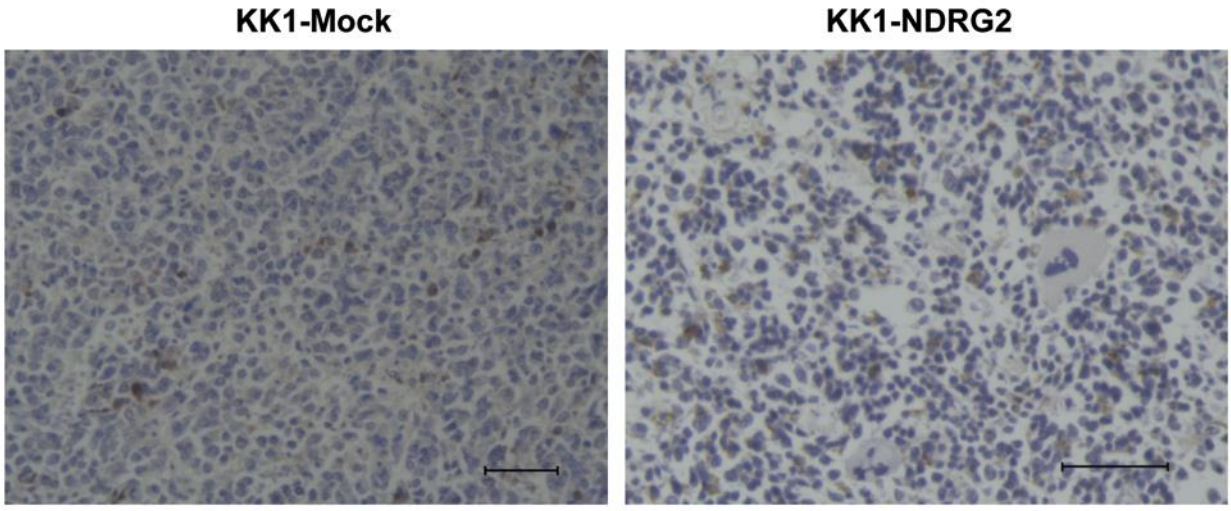

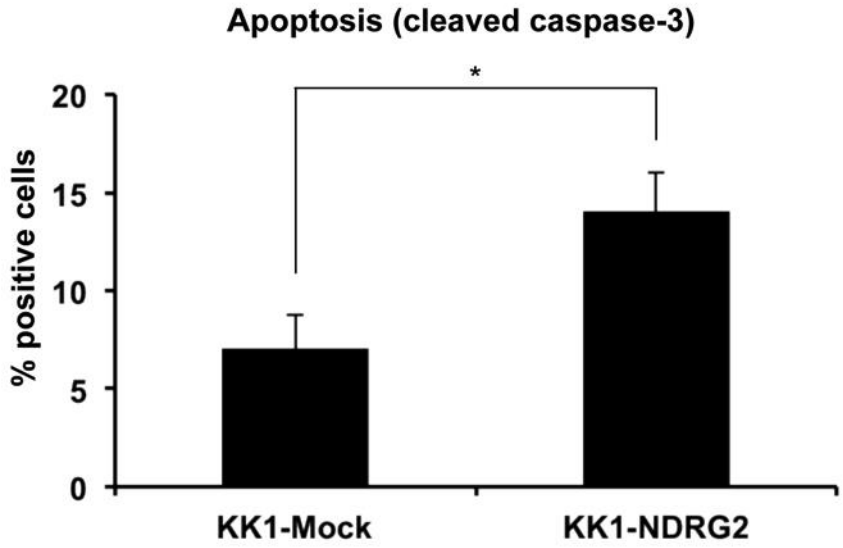

Supplementary Figure 9. Neoplastic cells from KK1-NDRG2-injected NOG mice had a higher rate of apoptosis than those from KK1-Mock-injected NOG mice. Tissue sections in Supplementary Fig. 8c,e were immunostained with anti-cleaved caspase-3 antibody and the percentage of apoptotic cells was quantified by counting the number of cleaved caspase-3 immunostained cells and expressing as a percentage of the total cells. The mean±s.d. is shown, $*P < 0.05$ (Student's *t* test). The data are representative of two experiments. Scale bar, 50 μm.

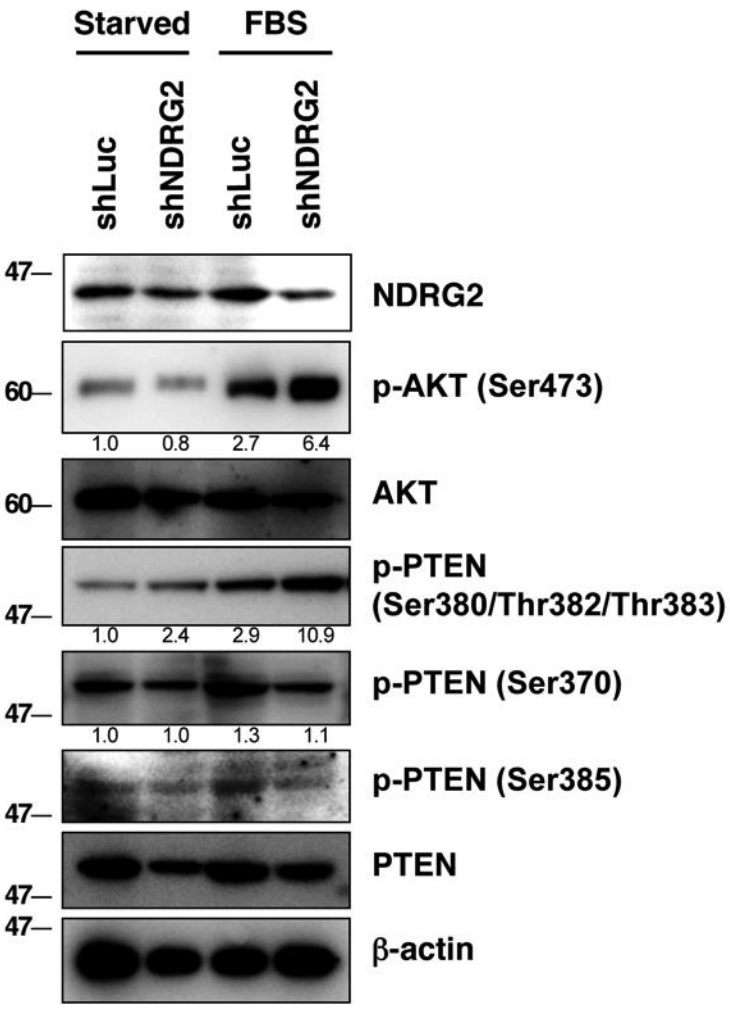

Supplementary Figure 10. Suppression of NDRG2 expression in NIH3T3 cells enhances serum-induced phosphorylation of PTEN at Ser380/Thr382/Thr383 and AKT at Ser473. At 24 h after transfection with the shNDRG2 or shLuc expression vectors into NIH3T3 cells, the cells were starved in medium containing 1% FBS for 16 h, treated with or without 10% FBS for 24 h, and analysed for protein levels of NDRG2, total PTEN, phosphorylated PTEN (Ser370, Ser380/Thr382/Thr383 cluster, and Ser385), total AKT, and phosphorylated AKT (Ser473). The value is the ratio of the band density of phosphorylated AKT and phosphorylated PTEN divided by the band density of the corresponding AKT and PTEN, respectively. Data are representative of two experiments.

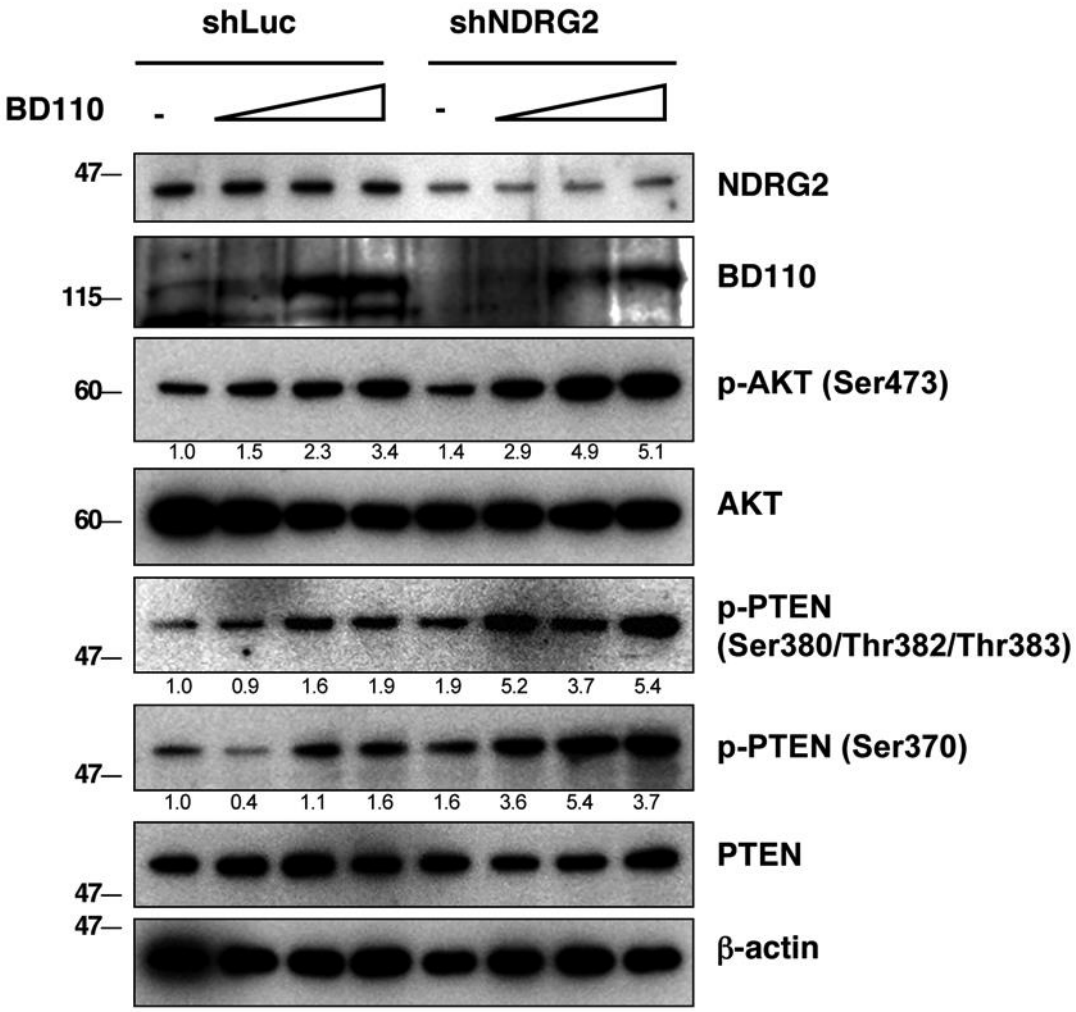

Supplementary Figure 11. Suppression of NDRG2 expression in NIH3T3 cells enhances constitutively active mutant PI3K-induced phosphorylation of PTEN at Ser380/Thr382/Thr383. At 24 h after transfection with the shNDRG2 or shLuc expression vectors into NIH3T3 cells, the cells were additionally transfected with increasing amounts of constitutive active PI3K (BD110) plasmid (0.25, 0.5, and 1 μg). Following 24 h of incubation, the cells were analysed for protein levels of NDRG2, total PTEN, phosphorylated PTEN (Ser370 and Ser380/Thr382/Thr383 cluster), total AKT, and phosphorylated AKT (Ser473). Myc-pBD110 was detected by an anti-Myc tag antibody. Assays were performed in the presence of complete growth medium. The value is the ratio of the band density of phosphorylated AKT and phosphorylated PTEN divided by the band density of the corresponding AKT and PTEN, respectively. The data are representative of two experiments.

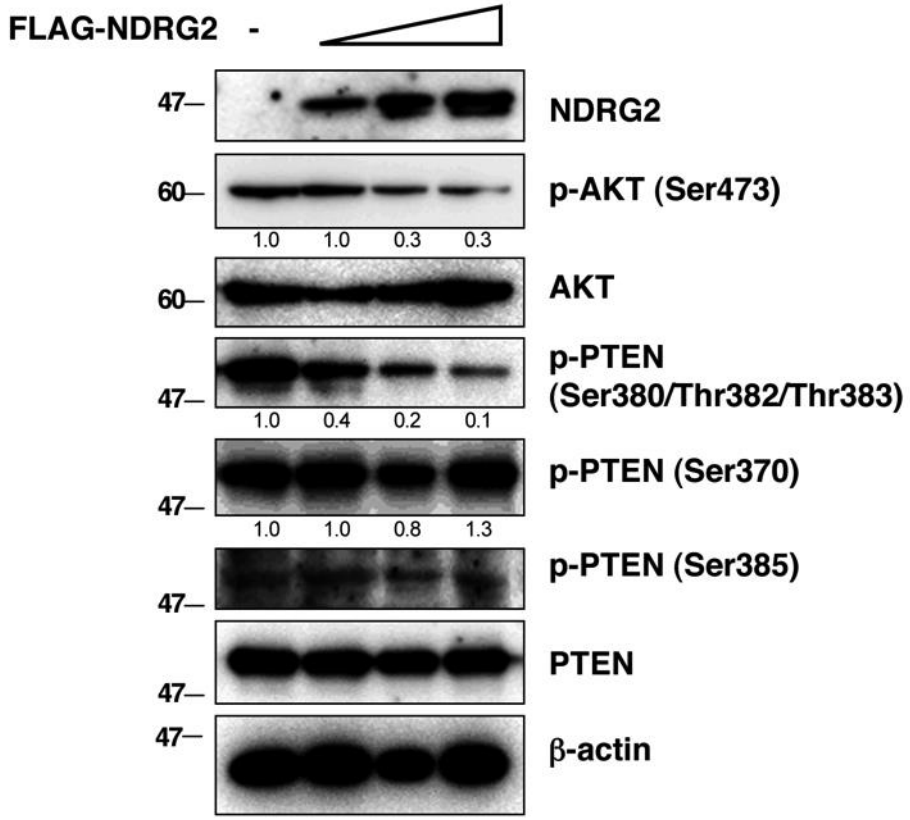

Supplementary Figure 12. Overexpression of NDRG2 in NIH3T3 cells attenuates the phosphorylation of PTEN at Ser380/Thr382/Thr383 and AKT at Ser473. After transfection with increasing amounts of FLAG-NDRG2 expression vector (0.5, 1.5, and 4.5 μg) and incubation for 48 h, the cells were analysed for protein levels of NDRG2, total PTEN, phosphorylated PTEN (Ser370, Ser380/Thr382/Thr383 cluster, and Ser385), total AKT, and phosphorylated AKT (Ser473). Assays were performed in the presence of complete growth medium. The value is the ratio of the band density of phosphorylated AKT and phosphorylated PTEN divided by the band density of the corresponding AKT and PTEN, respectively. The data are representative of two experiments.

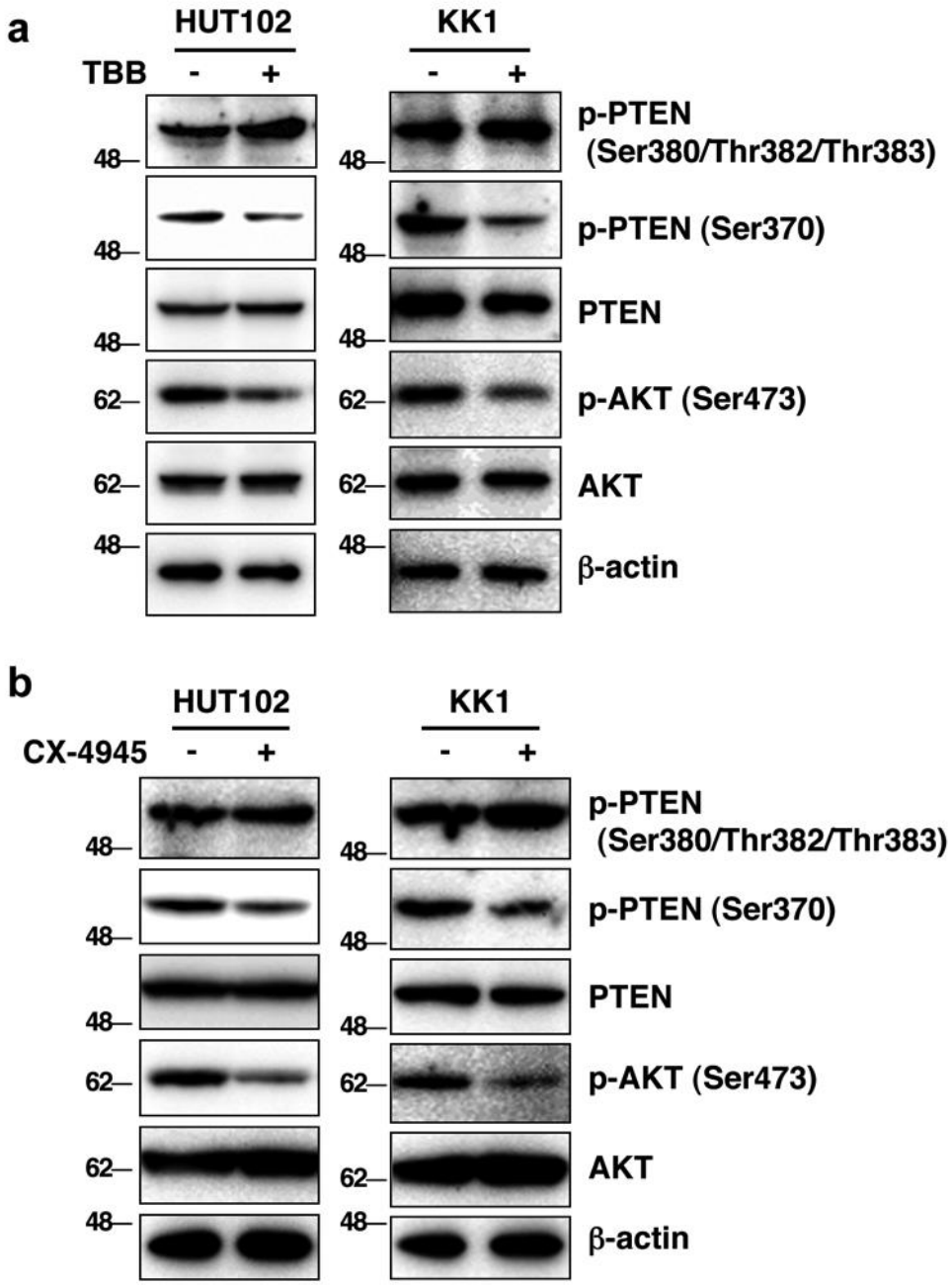

Supplementary Figure 13. CK2 is not responsible for PTEN-Ser380/Thr382/Thr383 phosphorylation in ATLL cells. (**a**) HUT102 and KK1 cells were treated with DMSO or 20 μM TBB for 24 h and analysed for protein levels of total PTEN, phosphorylated PTEN (Ser370 and Ser380/Thr382/Thr383 cluster), total AKT, and phosphorylated AKT (Ser473). (**b**) HUT102 and KK1 cells were treated with DMSO or 1 μM CX-4945 for 24 h and subjected to Western blot analysis with the same antibodies as in a. The data are representative of three experiments.

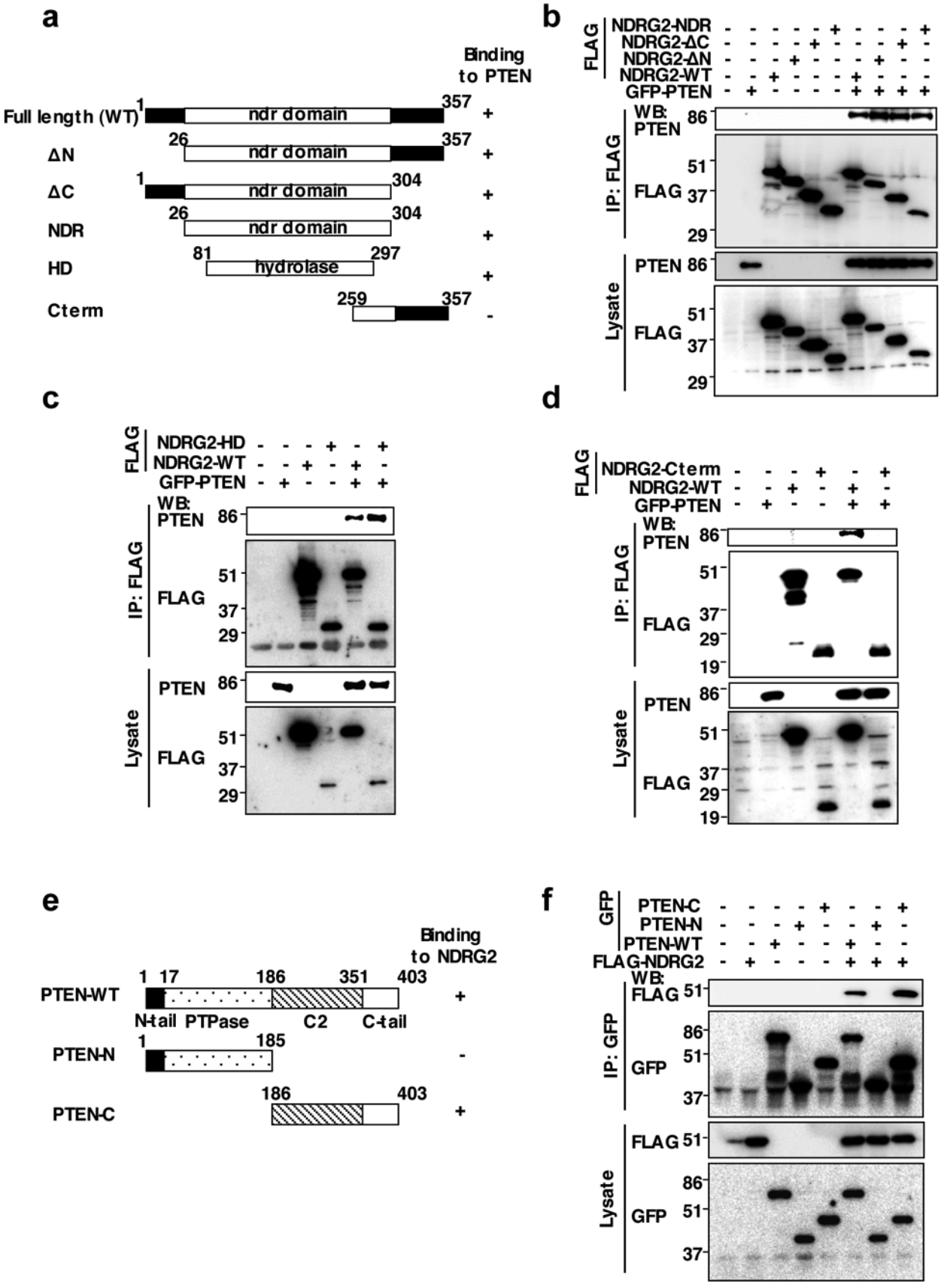
a
Binding to PTEN
Full length (WT)
1
357
ndr domain
+
ΔN
26
357
ndr domain
+
ΔC
1
304
ndr domain
+
NDR
26
304
ndr domain
+
HD
81
297
hydrolase
+
Cterm
259
357
-
b
FLAG
NDRG2-NDR
NDRG2-ΔC
NDRG2-ΔN
NDRG2-WT
GFP-PTEN
IP: FLAG
WB: PTEN
FLAG
Lysate
PTEN
FLAG
86
51
37
29
c
FLAG
NDRG2-HD
NDRG2-WT
GFP-PTEN
IP: FLAG
WB: PTEN
FLAG
Lysate
PTEN
FLAG
86
51
37
29
d
FLAG
NDRG2-Cterm
NDRG2-WT
GFP-PTEN
IP: FLAG
WB: PTEN
FLAG
Lysate
PTEN
FLAG
86
51
37
29
19
e
Binding to NDRG2
PTEN-WT
1
17
186
351
403
+
N-tail
PTPase
C2
C-tail
PTEN-N
1
185
-
PTEN-C
186
403
+
f
GFP
PTEN-C
PTEN-N
PTEN-WT
FLAG-NDRG2
IP: GFP
WB: FLAG
GFP
Lysate
FLAG
GFP
86
51
37

Supplementary Figure 14. Mapping of the binding domains involved in the interaction between NDRG2 and PTEN. (**a**) Domain structure of the full-length NDRG2 and the NDRG2 deletion mutants used for the *in vitro* binding assay. (**b-d**) 293T cells were transiently transfected with various types of FLAG-tagged NDRG2 constructs and/or GFP-PTEN. After 48 h, the whole cell lysates were immunoprecipitated with an anti-FLAG antibody, and the immunoprecipitates were immunoblotted by anti-FLAG or anti-PTEN antibodies to detect NDRG2 or PTEN, respectively. (**e**) Domain structure of the full-length PTEN and the PTEN deletion mutants. (**f**) After transfection with various types of GFP-tagged PTEN constructs and/or FLAG-NDRG2 into 293T cells, the whole cell lysates were immunoprecipitated by an anti-GFP antibody. The precipitates were immunoblotted by anti-GFP or anti-FLAG antibodies to detect PTEN or NDRG2, respectively. All data are representative of at least two experiments.

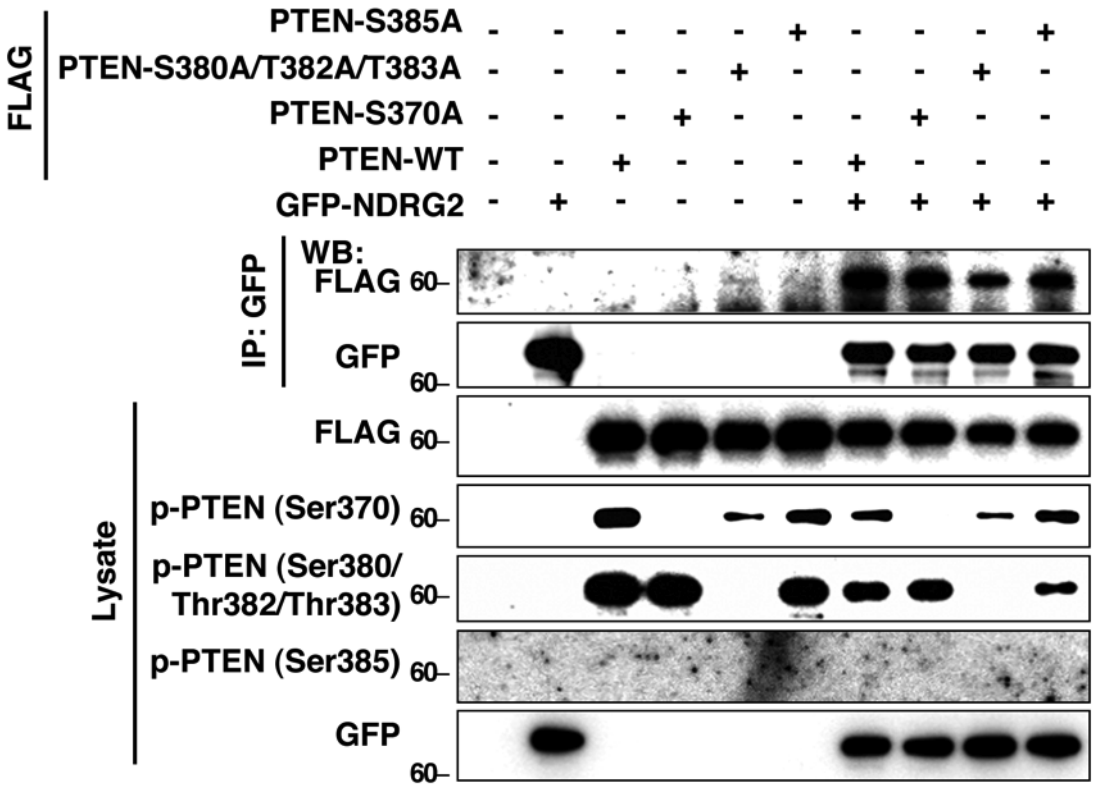

Supplementary Figure 15. The S370A, S380A/T382A/T383A, or S385A mutations in PTEN do not significantly change the binding affinity for NDRG2. 293T cells were transiently transfected with GFP-NDRG2 and/or FLAG-tagged-wild-type PTEN or -PTEN mutants (S370A, S380A/T382A/T383A, or S385A). After 48 h, the whole cell lysates were immunoprecipitated with an anti-GFP antibody, and the immunoprecipitates were immunoblotted by anti-FLAG or anti-GFP antibodies to detect PTEN or NDRG2, respectively. The lysates were probed for phosphorylated PTEN (Ser370, Ser380/Thr382/Thr383 cluster, and Ser385), total PTEN (FLAG), and NDRG2 (GFP). The data are representative of two experiments. Note that we observed no detectable signal with phosphorylated PTEN-Ser385.

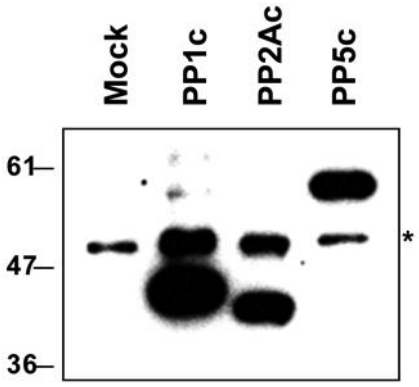

Supplementary Figure 16. Western blot analysis confirmed anti-Myc immunoprecipitation of lysates from 293T cells transfected with Myc-tagged PP1c, PP2Ac, and PP5c. The immunoprecipitates were analysed by immunoblotting with an anti-Myc antibody (Asterisk, IgG).

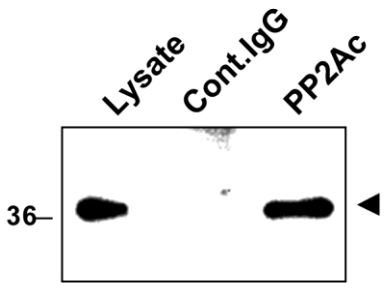

Supplementary Figure 17. Western blot analysis confirmed the anti-PP2Ac immunoprecipitation of lysates from NIH3T3 cells. The immunoprecipitates were analysed by immunoblotting with an anti-PP2Ac antibody. The arrowhead indicates PP2Ac protein.

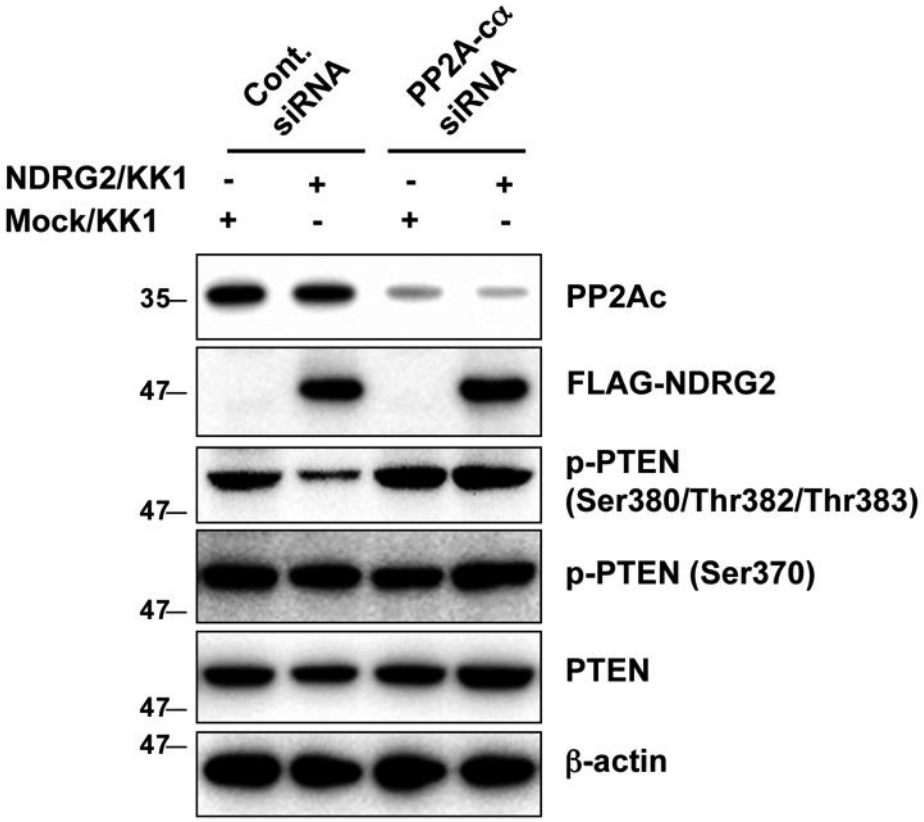

Supplementary Figure 18. The NDRG2-dependent down-regulation of PTEN-Ser380/Thr382/Thr383 phosphorylation was abrogated by siRNA-mediated knockdown of PP2Ac. KK1-NDRG2 or KK1-Mock cells were transiently transfected with NDRG2 or control siRNAs and analysed for protein levels of PP2Ac, NDRG2 (FLAG), total PTEN, and phosphorylated PTEN (Ser370 and Ser380/Thr382/Thr383 cluster). The data are representative of two experiments.

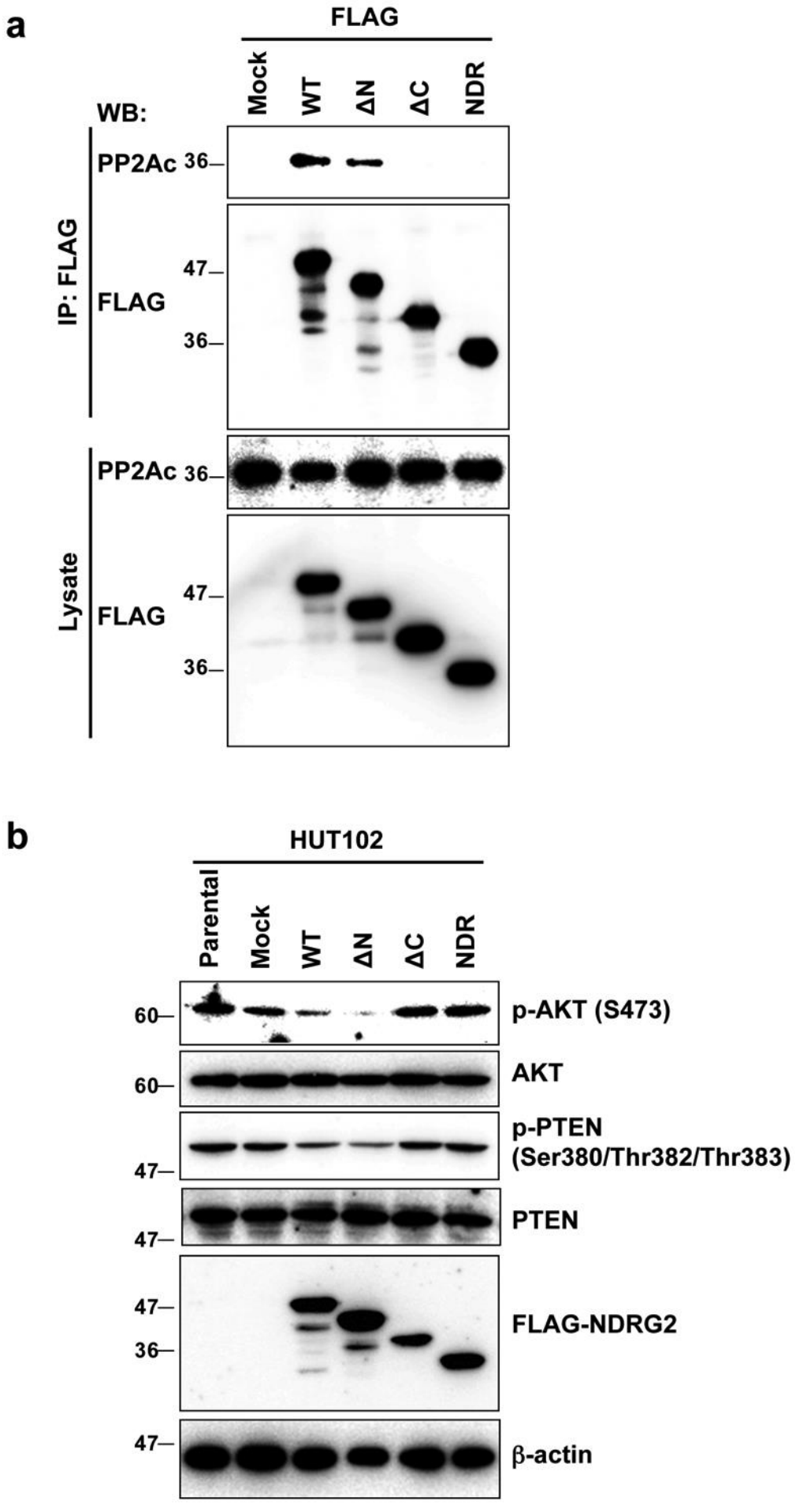
a
FLAG
Mock
WT
ΔN
ΔC
NDR
WB:
IP: FLAG
PP2Ac
36
FLAG
47
36
Lysate
PP2Ac
36
FLAG
47
36
b
HUT102
Parental
Mock
WT
ΔN
ΔC
NDR
60
p-AKT (S473)
60
AKT
p-PTEN
(Ser380/Thr382/Thr383)
47
PTEN
47
47
36
FLAG-NDRG2
47
β-actin

Supplementary Figure 19. The NDRG2 deletion mutants that fail to bind PP2A lose the ability to promote PTEN-Ser380/Thr382/Thr383 dephosphorylation. (**a**) 293T cells were transiently transfected with various types of FLAG-tagged NDRG2 constructs (Supplementary Figure 14a). After 48 h, cells were treated with the cross-linker DTBP, and the cell lysates were immunoprecipitated with an anti-FLAG antibody, followed by immunoblotting with anti-FLAG or anti-PP2Ac antibodies. The data are representative of two experiments. (**b**) HUT102 cells were transiently transfected with the same construct used in a and analysed for protein levels of NDRG2 (FLAG), total PTEN, phosphorylated PTEN (Ser380/Thr382/Thr383 cluster), total AKT, and phosphorylated AKT (Ser473). The data are representative of two experiments.

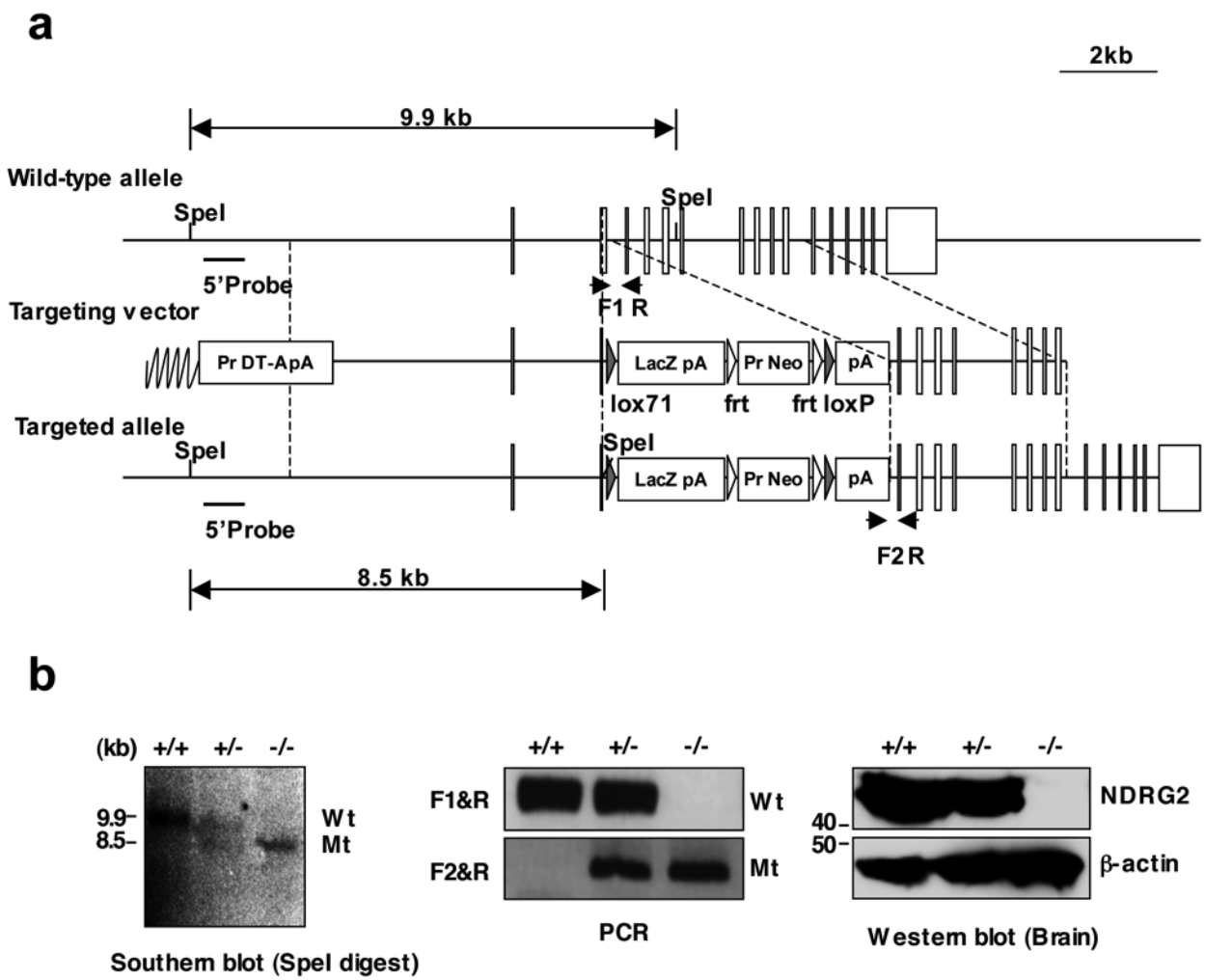

Supplementary Figure 20. Generation of *NDRG2*-deficient mice. (**a**) Schematic of the *NDRG2* gene targeting strategy. Structure of the wild-type *NDRG2* allele (top), the targeting vector (middle), and the predicted targeted allele (bottom). The *lacZ*-pA-*neo*-pA cassette was inserted into exon 2 (the first coding exon) of the *NDRG2* gene. The position of *Spe*I-sites, the location of the PCR primers (F1, F2, and R, small arrows) used to screen for homologous recombination, and the 5' probe (short horizontal bar) used for the Southern blot analysis are shown. (**b**) Mouse genotyping by Southern blot, PCR, and Western blot analyses. Genomic DNA from mouse tail was digested with *Spe*I and hybridized with the 5' probe. The wild-type allele gave a 9.9-kb band, whereas the targeted allele gave an 8.5-kb band. PCR amplification of the wild-type (F1&R) and the targeted (F2&R) alleles resulted in products of 224 bp and 414 bp, respectively. Whole brain homogenates

from wild-type, heterozygous, and homozygous mice were subjected to Western blotting using anti-NDRG2 and anti-β-actin antibodies.

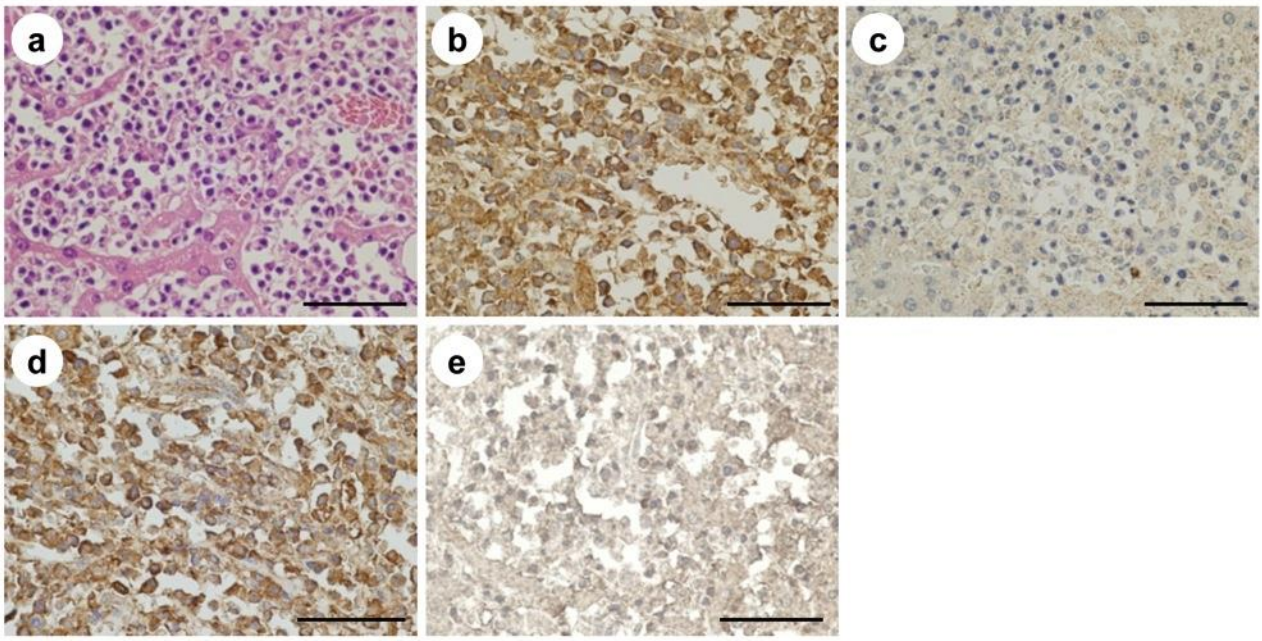

Supplementary Figure 21. The histopathological findings of *NDRG2*-deficient mice. Tumour sections from the liver of an *NDRG2*$^{+/-}$ mouse were subjected to histopathology. The results demonstrated massive infiltration of large atypical lymphoid cells in portal areas and the sinus of the liver. The tumour cells were positive for CD3 (b) and CD4 (d) but negative for CD8 (e) and B220 (c). a. H&E staining. Scale bar, 100 μm.

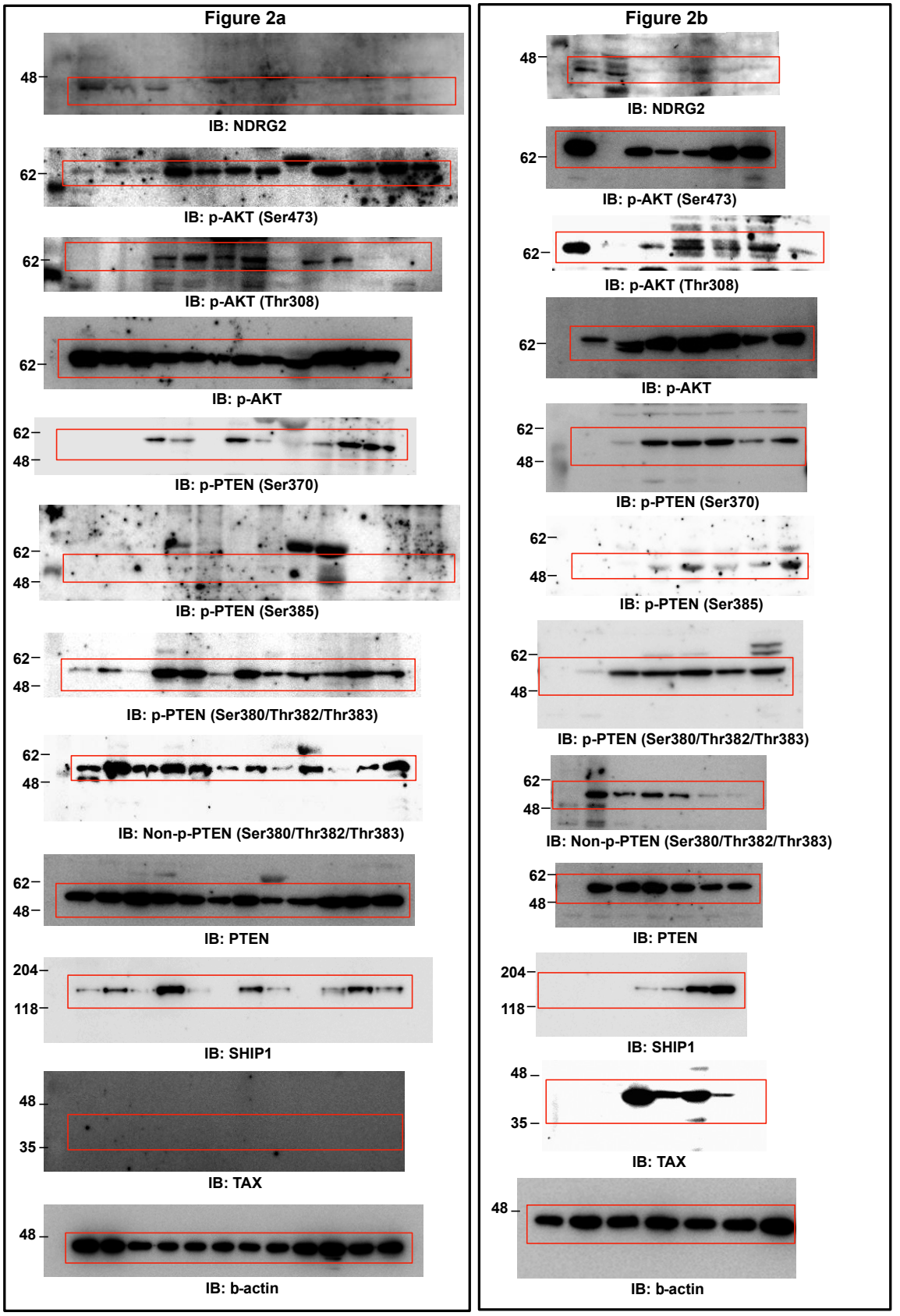
Figure 2a
48
IB: NDRG2
62
IB: p-AKT (Ser473)
62
IB: p-AKT (Thr308)
62
IB: p-AKT
62
48
IB: p-PTEN (Ser370)
62
48
IB: p-PTEN (Ser385)
62
48
IB: p-PTEN (Ser380/Thr382/Thr383)
62
48
IB: Non-p-PTEN (Ser380/Thr382/Thr383)
62
48
IB: PTEN
204
118
IB: SHIP1
48
35
IB: TAX
48
IB: b-actin
Figure 2b
48
IB: NDRG2
62
IB: p-AKT (Ser473)
62
IB: p-AKT (Thr308)
62
IB: p-AKT
62
48
IB: p-PTEN (Ser370)
62
48
IB: p-PTEN (Ser385)
62
48
IB: p-PTEN (Ser380/Thr382/Thr383)
62
48
IB: Non-p-PTEN (Ser380/Thr382/Thr383)
62
48
IB: PTEN
204
118
IB: SHIP1
48
35
IB: TAX
48
IB: b-actin

Supplementary Figure 22. Western blot images of the selected portion displayed in Fig. 2a,b, Fig. 5g,h, Fig. 6a-d, and Fig. 7c,d.

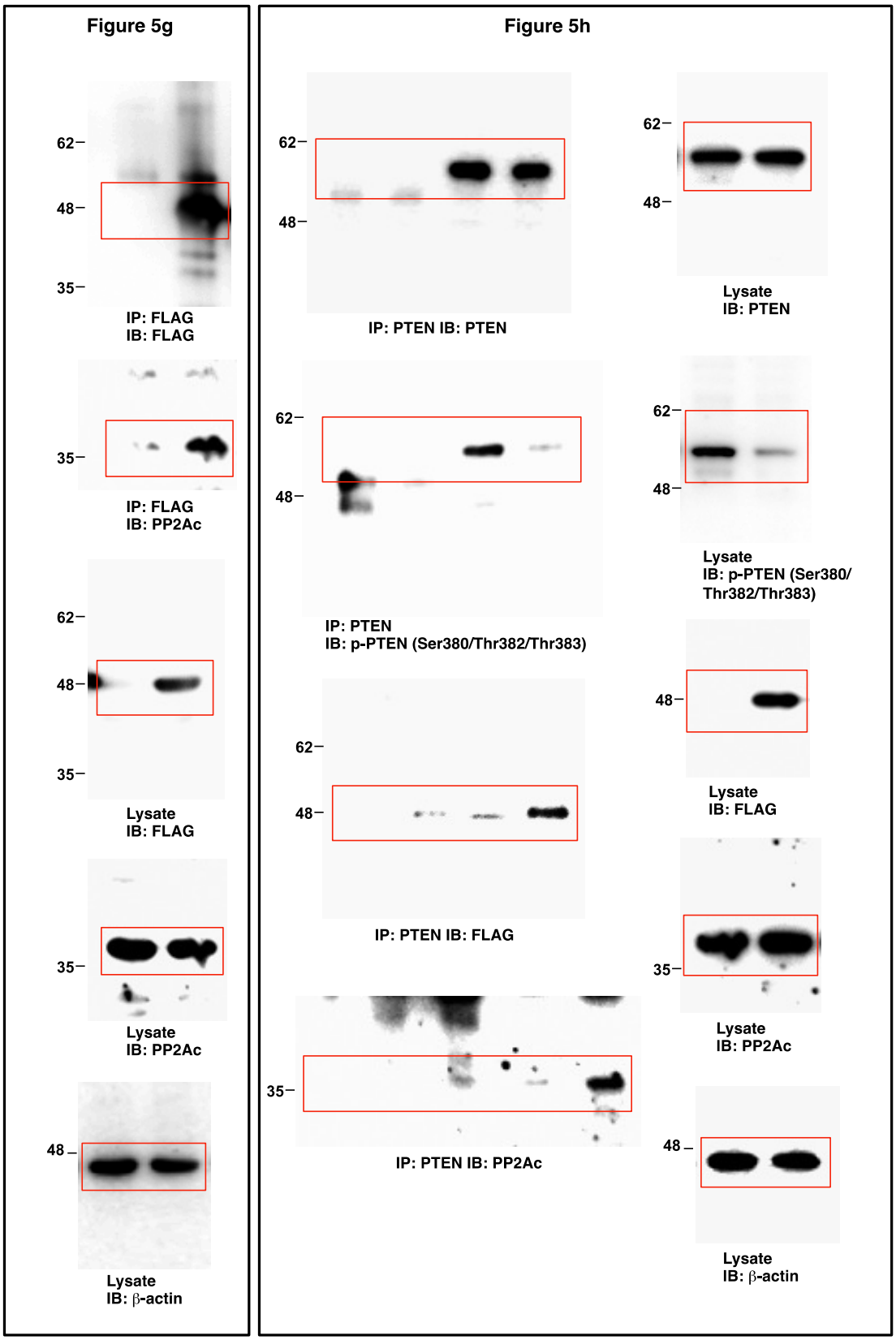

Supplementary Figure 22 (continued)

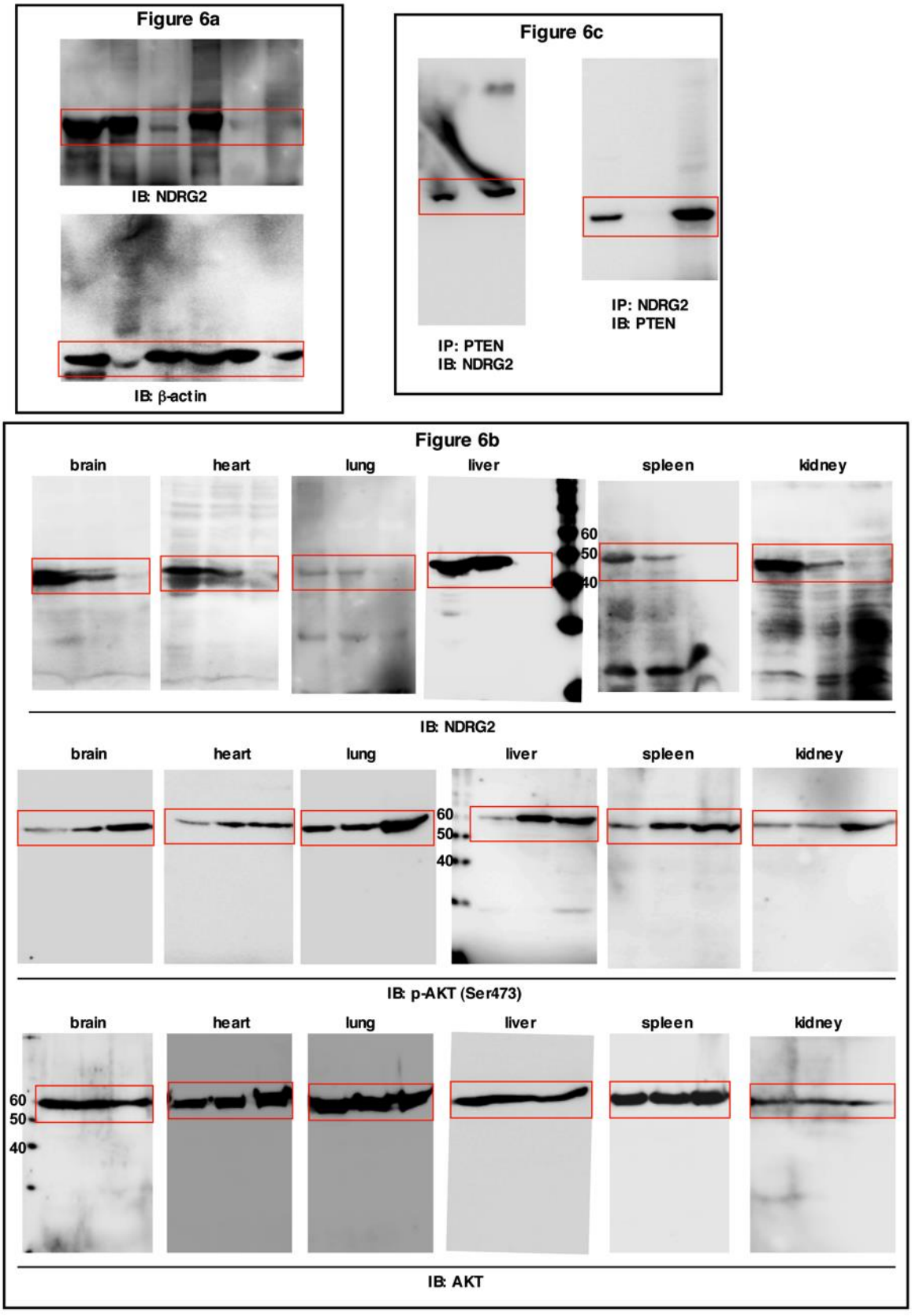

Supplementary Figure 22 (continued)

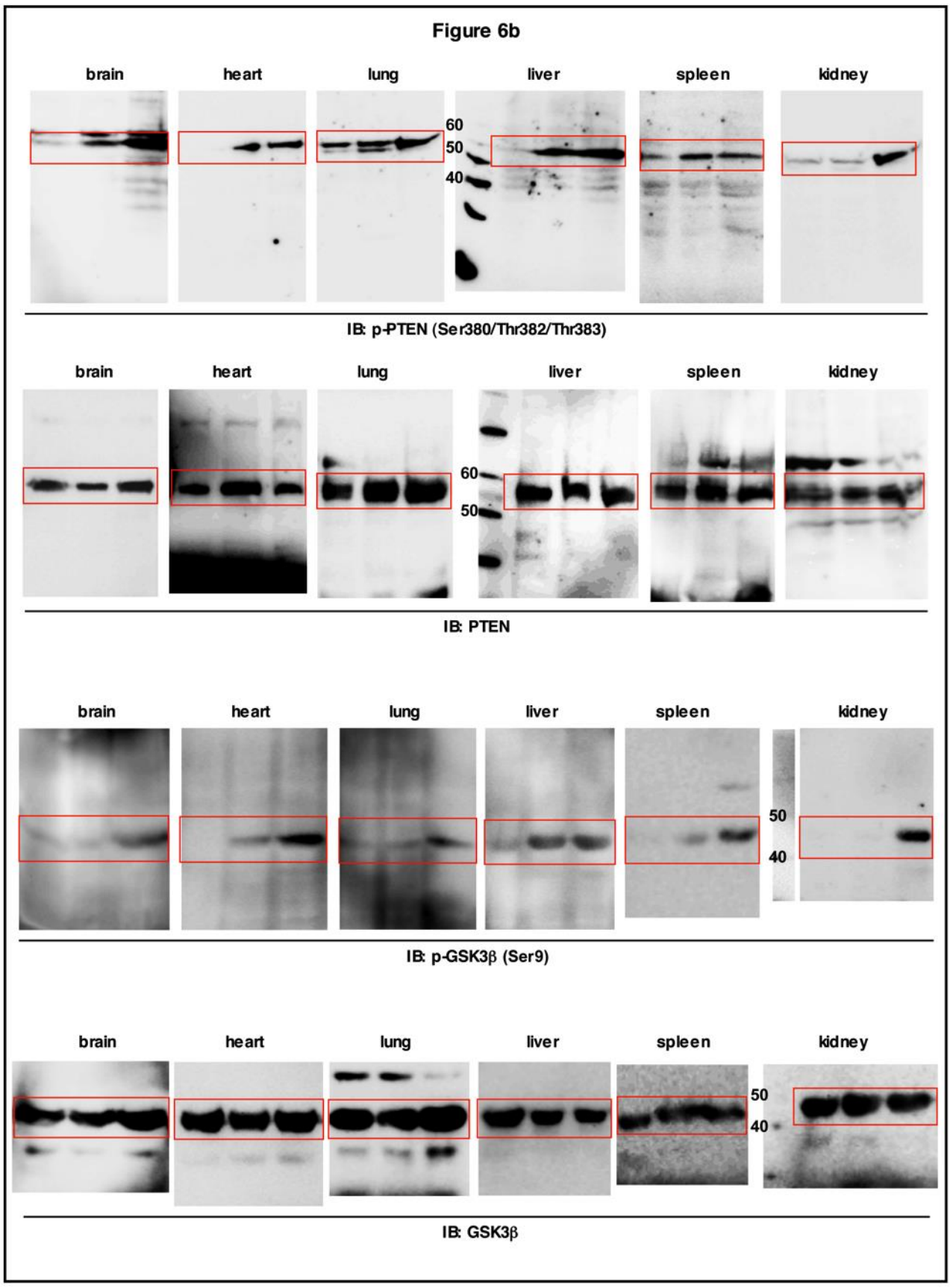

Supplementary Figure 22 (continued)

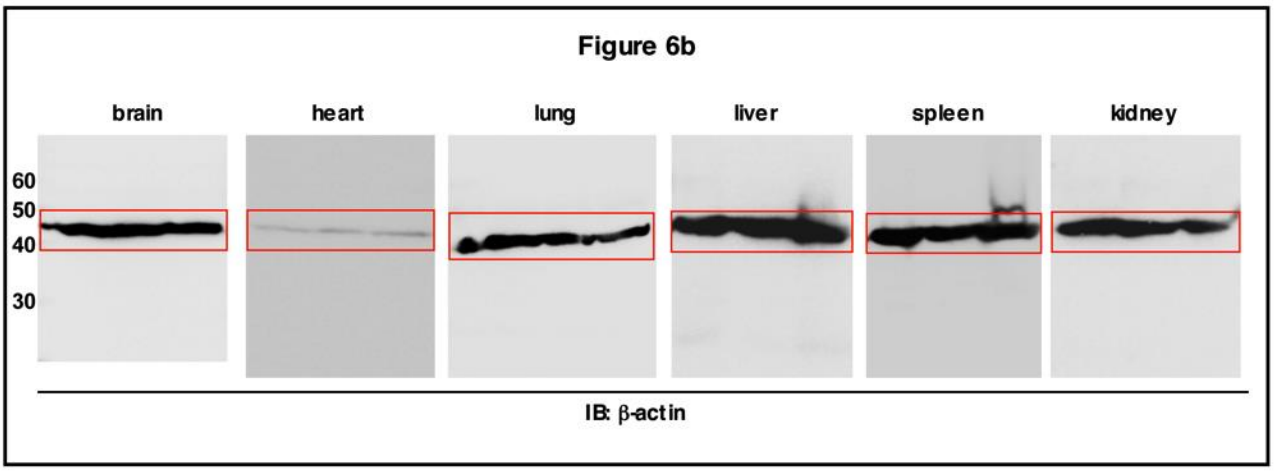

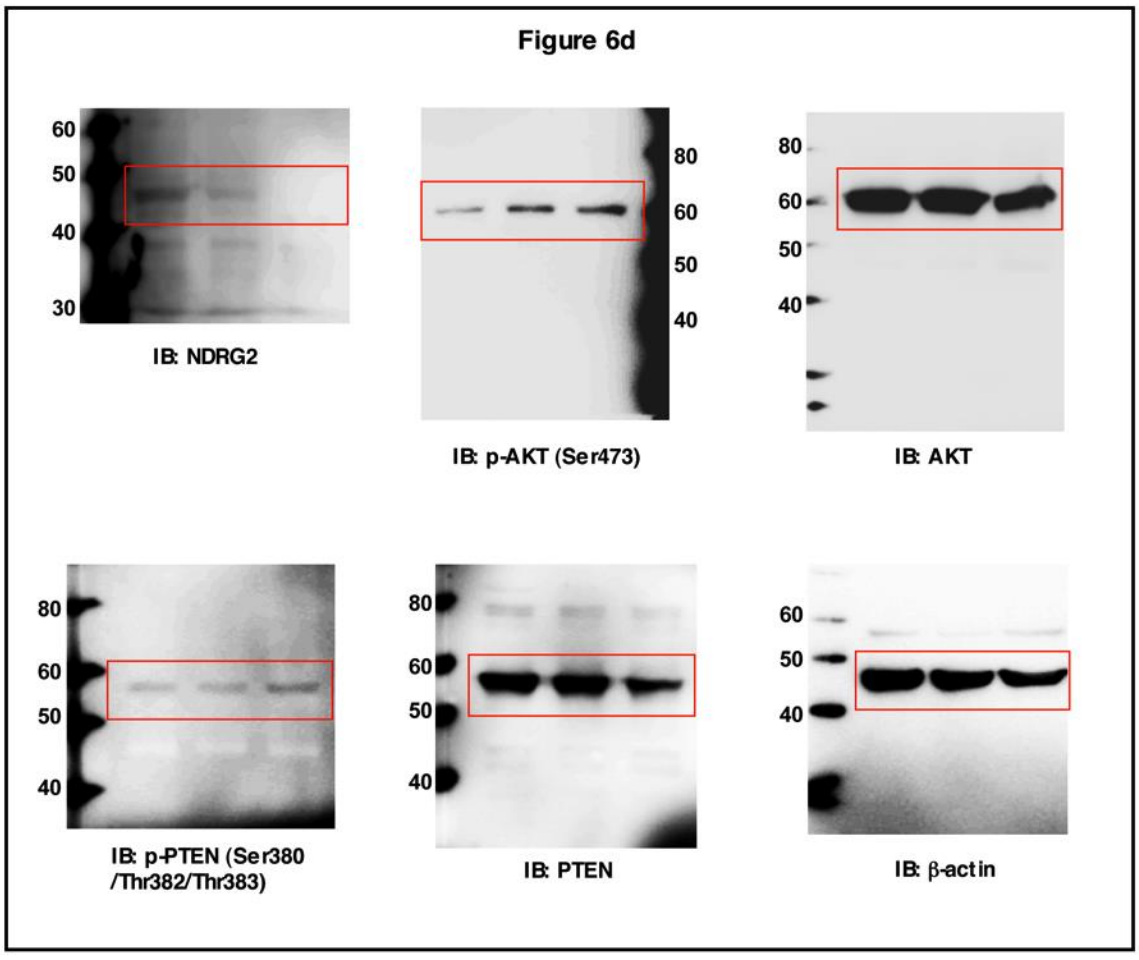

Supplementary Figure 22 (continued)

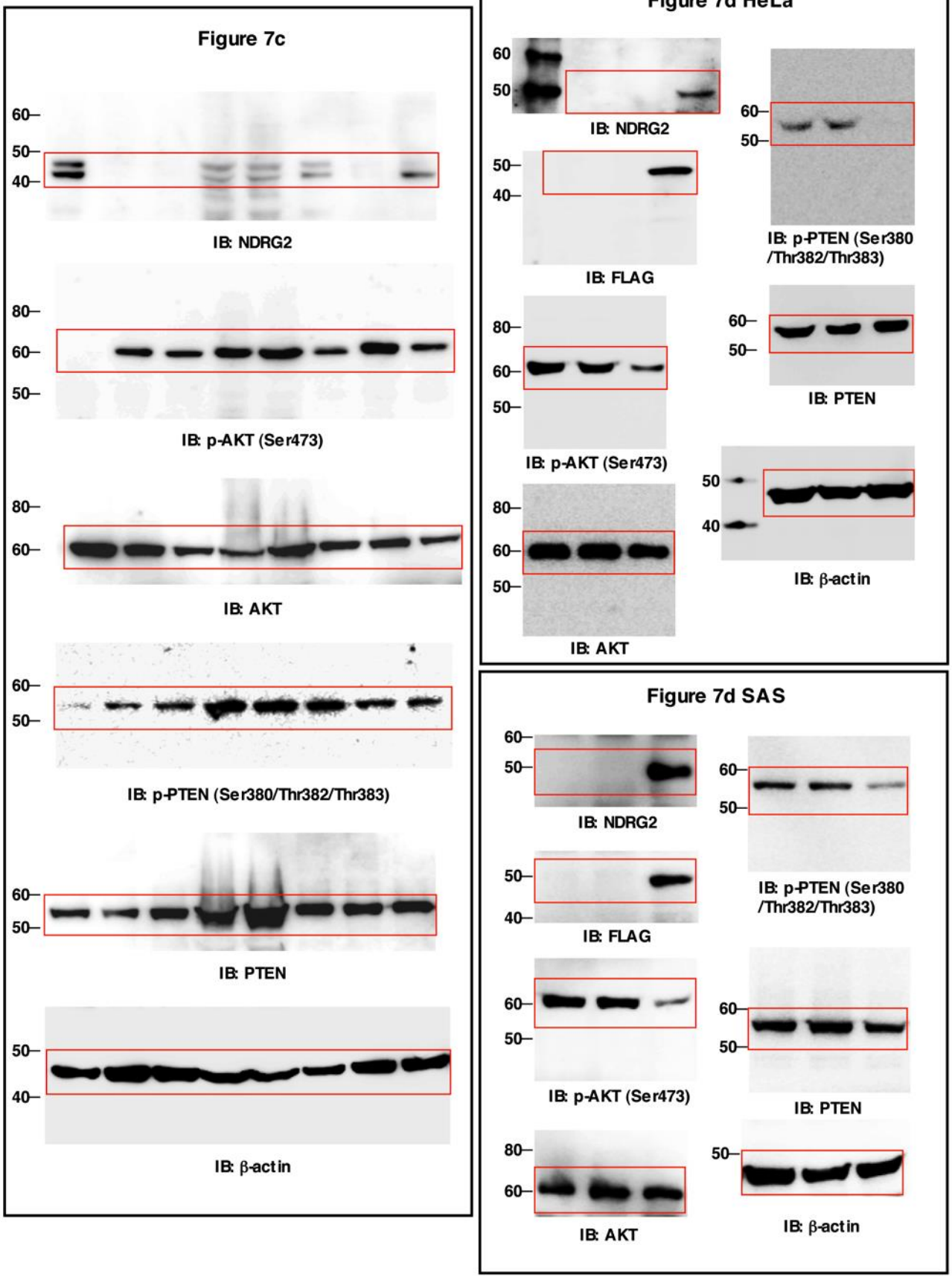

Supplementary Figure 22 (continued)

Supplementary Table 1. The list of genes methylated and silenced in association with the progression of the disease.

Gene symbol	Fold changes in gene expression in various types of ATLL				Average methylation beta values in various types of ATLL			
	Smoldering-type	Chronic-type	Acute-type		CD4+ lymphocytes	Smoldering-type	Chronic-type	Acute-type
PDE4DIP	0.537	0.487	0.431		0.082	0.515	0.594	0.809
ADAM15	0.606	0.568	0.327		0.049	0.066	0.088	0.171
RORC	0.118	0.093	0.053		0.756	0.823	0.805	0.876
ENAH	0.478	0.454	0.406		0.063	0.196	0.384	0.528
BCL2L11	0.649	0.302	0.297		0.062	0.221	0.447	0.456
MAL	0.572	0.466	0.290		0.422	0.741	0.691	0.847
IL1RL1	0.357	0.346	0.119		0.768	0.820	0.842	0.876
ADD2	0.390	0.362	0.249		0.083	0.298	0.460	0.587
PTPN4	0.455	0.281	0.274		0.081	0.145	0.123	0.189
MBNL1	0.443	0.264	0.238		0.436	0.774	0.806	0.894
FNDC3B	0.487	0.476	0.323		0.129	0.387	0.463	0.644
FAM19A1	0.423	0.187	0.129		0.091	0.344	0.577	0.757
TTC14	0.507	0.490	0.428		0.488	0.632	0.576	0.725
FOXP1	0.416	0.411	0.290		0.053	0.087	0.097	0.157
ZNF595	0.518	0.428	0.408		0.594	0.678	0.694	0.720
ZNF354B	0.404	0.337	0.290		0.020	0.078	0.141	0.129
NPR3	0.612	0.521	0.478		0.031	0.254	0.388	0.604
TCF7	0.290	0.255	0.214		0.057	0.319	0.377	0.662
TOP1MT	0.500	0.363	0.335		0.381	0.504	0.547	0.590
GALNT12	0.383	0.377	0.231		0.297	0.753	0.823	0.943
PSIP1	0.553	0.516	0.420		0.747	0.830	0.810	0.886
MLLT10	0.694	0.616	0.528		0.109	0.183	0.208	0.242
PLEKHA1	0.418	0.340	0.296		0.107	0.460	0.635	0.688
ARHGAP22	0.434	0.417	0.349		0.074	0.239	0.311	0.494
NMT2	0.397	0.204	0.117		0.063	0.073	0.079	0.210
NDRG2	0.215	0.198	0.197		0.221	0.442	0.553	0.556
SNRPN	0.553	0.515	0.346		0.513	0.749	0.834	0.935
BNIP2	0.743	0.684	0.563		0.444	0.776	0.799	0.801
PITPNC1	0.268	0.253	0.195		0.719	0.833	0.862	0.873
MAP3K3	0.728	0.704	0.504		0.453	0.703	0.761	0.784
TNRC6C	0.812	0.663	0.620		0.677	0.673	0.809	0.861
LOC339290	0.763	0.619	0.554		0.034	0.095	0.210	0.212
ZNF528	0.431	0.378	0.333		0.305	0.561	0.664	0.793
ZNF358	0.661	0.625	0.563		0.024	0.118	0.395	0.496

A total of 34 genes were selected by the following criteria: (i) the degree of DNA methylation of the gene promoter region gradually increased and the mRNA abundance gradually decreased during the development of ATLL (from the smoldering/chronic stage to the acute stage), (ii) there was a negative correlation between gene expression and DNA methylation (Pearson r; $-1 < r \leq -0.5$), and (iii) the gene is differentially methylated and expressed with a P value < 0.1 (by the Cuzick test and t test, respectively) compared with the control group.

Fold change values are calculated by dividing the diseased group values by the control (normal $CD4^+$ lymphocytes) values.

Four patients with smoldering-type ATLL, six patients with chronic-type ATLL, eight patients with acute-type ATLL, and five healthy volunteers were included in the gene expression analysis.

Nine patients with smoldering-type ATLL, 10 patients with chronic-type ATLL, nine patients with acute-type ATLL, and five healthy volunteers were included in the DNA methylation analysis.

Supplementary Table 2. Methylation status of the promoter region of *NDRG2* as determined by MSP in leukaemia cell lines and primary leukaemia cells.

	Cell lines			Primary samples				
	T-ALL	ATLL	AML	PBL	ATLL	AML	T cell lymphoma	B cell lymphoma
Methylated	0	7	0	0	30	0	0	0
Partially methylated	0	1	1	0	4	1	1	0
Unmethylated	4	0	6	11	0	9	6	10
Total numbers (% methylation)	4 (0)	8 (100)	7 (14)	11 (0)	34 (100)	10 (10)	7 (14)	10 (0)

The cell lines used included four T-ALL cell lines (Jurkat, MOLT4, KAWAI, and MKB-1), eight ATLL cell lines (MT-2, HUT102, ED, SO4, Su9T01, S1T, KK1, and KOB), and seven acute myeloid leukaemia (AML) cell lines (UCSD/AML1, Kasumi-3, OIH-1, K051, NH, MOLM1, and FKH-1). Primary samples were obtained from 11 healthy volunteers (peripheral blood lymphocytes, PBL), ATLL cells from 34 patients with acute-type ATLL, AML cells from 10 patients, and tumour cells from lymph nodes from 7 patients with T-lymphoma and from 10 patients with B-lymphoma. The MT-2 cell line showed partial methylation in the *NDRG2* promoter, but after treatment with 5-aza-dC, an increase in *NDRG2* mRNA abundance could not be detected (Supplementary Fig. 1).

Supplementary Table 3. Frequency of *NDRG2*, *PTEN*, and *PIK3CA* mutations in different types of cancer cell lines and primary ATLL cases.

	NDRG2 Mutations			*PTEN* Mutations			*PIK3CA* Mutations		
Cell lines	-	+	Total	-	+	Total	-	+	Total
T-ALL	4	0	4	3	1 ins/del241 stop, ins247stop	4	4	0	4
ATLL	8	0	8	8	0	8	8	0	8
AML			nd	7	0	7			nd
Pancreatic cancer	3	0	3	3	0	3	3	0	3
Glioblastoma	1	0	1	0	1 Y68H, F81S, L182N, L186N	1	0	1 H1047R	1
Neuroblastoma	2	0	2	2	0	2	2	0	2
Liver cancer	4	0	4	4	0	4	4	0	4
OSCC	7	1 A336S	8	8	0	8	6	1 H1047R	7
Gastric cancer	3	0	3	3	0	3	3	0	3
Breast cancer	1	0	1	1	0	1	1	0	1
Colon cancer	1	0	1	1	0	1	1	0	1
Ovarian cancer	1	0	1	1	0	1	0	1 H1047R	1
Prostate cancer	1	0	1	0	1 F341V	1	1	0	1
Cervical cancer	1	0	1	1	0	1	0	1 H1047R	1
Lung cancer	5	0	5	5	0	5	1	0	1
Total Numbers	42	1	43	47	3	50	34	4	38
Primary samples									
ATLL	34	0	34	34	0	34	34	0	34

Values are numbers of cases.

The cell samples used included four T-ALL cell lines (Jurkat, MOLT4, KAWAI, and MKB-1), eight ATLL cell lines (MT-2, HUT102, ED, SO4, Su9T01, S1T, KK1, and KOB), seven AML cell lines (UCSD/AML1, Kasumi-3, OIH-1, K051, NH, MOLM1, and FKH-1), three pancreatic cancer cell lines (KLM1, PK9, and PK45P), one glioblastoma cell line (A172), two neuroblastoma cell lines (NH6 and NH12), four hepatic cancer cell lines (HepG2, HuH7, HLF, and HuH28), eight oral squamous cell carcinoma (OSCC) cell lines (SAS, HO-1-U-1, Ca9-22, HSC2, HSC3, HSC4, HSQ89, and Sa3), three gastric cancer cell lines (Mkb28, Mkb45, and KatoIII), one breast cancer cell line (SK-BR-3), one colon cancer cell line (COLO205), one ovarian cancer cell line (SKOV3), one prostate cancer cell line

(PC3), one cervical cancer cell line (HeLa), five lung cancer cell lines (A549, H322, H1395, H1437, and H1648), and ATLL cells from 34 patients with acute-type ATLL (the same samples as those used in Supplementary Table 2).

nd: not determined.

Supplementary Table 4. Frequency of SNPs in the *NDRG2* gene.

Sequence variation	Reference SNP ID	Genotype frequency (%)		
-49 from the TSS C>A g2493824c	rs2297063	C/C = 86.8	C/A = 13.2	A/A = 0
IVS4 +78 C>G g2491162c	rs1243450	C/C = 34.2	C/G = 23.7	G/G = 42.1
exon9 371bp C>A g2488838c (124 Tyr to Ser)	rs4387520	C/C = 92.1	C/A = 7.9	A/A = 0
IVS15 -42 T>C g2486282c	rs1243446	T/T = 76.3	T/C = 21.1	C/C = 2.6
exon16 831bp T>C g2486227c (277 Ser to Ser)	rs4981349	C/C = 2.6	C/T = 10.5	T/T = 86.9
IVS17 +92 A>G g2485894c	rs1243444	A/A = 39.4	A/G = 39.5	G/G = 21.1

TSS, transcription start site; IVS, intron.

The cell samples used included eight ATLL cell lines (MT-2, HUT102, ED, SO4, Su9T01, S1T, KK1, and KOB) and ATLL cells from 30 patients with acute-type ATLL (the same samples as those used in Supplementary Table 2).

Supplementary Table 5. Offspring of heterozygous crosses.

	Genotype	Numbers of offspring	Percentage (%)
Male	WT (+/+)	23	25.0
	hetero (+/-)	42	45.7
	homo (-/-)	27	29.3
	total	92	48.7
Female	WT (+/+)	27	27.8
	hetero (+/-)	50	51.6
	homo (-/-)	20	20.6
	total	97	51.3
total	WT (+/+)	50	26.4
	hetero (+/-)	92	48.7
	homo (-/-)	47	24.9
	total	189	100

Percentages are calculated as the number of offspring with each genotype divided by the total number of offspring in each category.

Supplementary Table 6. Tumour incidence in *NDRG2*-deficient mice.

	WT (%)	*NDRG2* Chimera (%)	*NDRG2* hetero (%)	*NDRG2* homo (%)
Total number	15	10	31	12
Male	8	10	18	7
Female	7	0	13	5
Number of mice with tumours	4 (26.7)	5 (50)	20 (64.5)	9 (75)
Lymphoma	2 (13.3)	0	12 (38.7)	7 (58.3)
Lung cancer	1 (6.7)	3 (30)	4 (12.9)	1 (8.3)
Hepatic cancer	0	2 (20)	1 (3.2)	1 (8.3)
Intestinal cancer	0	0	1 (3.2)	0
Pancreatic cancer	0	0	1 (3.2)	0
Testicular cancer	0	1 (10)	1 (3.2)	0
Hemangioma/sarcoma	2 (13.3)	1 (10)	1 (3.2)	0
Skin tumour	0	2 (20)	1 (3.2)	0
Brain tumour	0	0	1 (3.2)	0
Total tumour number	5	9	23	9

Values are numbers of mice.

The numbers in parentheses are the percent incidences.

Note that the tumor incidence in *NDRG2*$^{+/-}$ and *NDRG2*$^{-/-}$ mice is significantly different from that in wild-type mice ($P < 0.05$, Fisher's exact test).

Supplementary Table 7. Methylation status of the promoter region of *NDRG2* as determined by MSP in different types of cancer cell lines.

	NDRG2 methylation		
Cell lines	Methylated	Partially methylated	Unmethylated
Pancreatic cancer	3	0	0
Glioblastoma	0	0	1
Neuroblastoma	0	0	2
Liver cancer	3	1	0
OSCC	8	0	0
Gastric cancer	3	0	0
Breast cancer	0	1	0
Colon cancer	1	0	0
Ovarian cancer	1	0	0
Prostate cancer	0	1	0
Cervical cancer	0	1	0
Lung cancer	1	0	0
Total numbers	20	4	3
Number of methylation positive (% methylation)		24 (89)	

The cell samples were the same as those used in Supplementary Table 3.

Supplementary Table 8. Oligonucleotides used for the mutagenesis of *PTEN*.

Primers	
S370A	CAGATGTTGCTGACAATGAACCTGATC
S380A/T382A/T383A	TATAGATATGCTGACGCCGCTGACTCTG
S385A	CACCACTGACGCTGATCCAGAGA

Supplementary Table 9. Primers for amplification of the *NDRG2* gene.

Primers	Forward	Reverse
exon4-5	GTGTTCTAGAGTAGTCTTCAACCCC	AGAGGGGAGAGATAGGGAAGGG
exon6-8	ACTCCCAGCTCCCTGACCTTG	GAGTTCAGAAGCTGAAACTGGCTC
exon9-11	GTCCTCCAAAGAAAGGTCCGTG	ATTGCACACTACCCAGACTTCCC
exon12-13	TTTAGACAAAGATAGTTCCATCATGGG	TTTGTTTTGTTCTTCGTTCACCCC
exon13-14	TGAACGAAGAACAAAACAAAGGGG	AATCAAAGATCAAGGTCATCTCCC
NDRG2 promo	CAGGTTTCCTTTTGCCTAAACAACTTC	CCCGCCCGAACACAGAGAAC

Supplementary Table 10. Primers for amplification of the *PTEN* gene.

Primers	Forward	Reverse
exon1	GGCATCAGCTACCGCCAAGT	CCAAACTACGGACATTTTCG
exon2	CTTTCTTTTCATAACTAGCTAATG	ATAATAGTTTACATCACAAAGTATC
exon3	TAATTTCAAATGTTAGCTCAT	AAGATATTTGCAAGCATACAA
exon4	GTTTGTTAGTATTAGTACTTT	ACAACATAGTACAGTACATTC
exon5-1	TATTCTGAGGTTATCTTTT	CTTTCCAGCTTTACAGTGAA
exon5-2	GCTAAGTGAAGATGACAATCA	AGGAAAAACATCAAAAAATAA
exon6	TTGGCTTCTCTTTTTTTCTG	ACATGGAAGGATGAGAATTTC
exon7	CCTGTGAAATAATACTGGTATG	CTCCCAATGAAAGTAAAGTACA
exon8-1	TTAAATATGTCATTTCATTTCTTTTTC	CTTTGTCTTTATTTGCTTTGT
exon8-2	GTGCAGATAATGACAAGGAATA	ACACATCACATACATACAAGTC
exon9	TTCATTTTAAATTTTCTTTCT	TGGTGTTTTATCCCTCTTGAT

Supplementary Table 11. Primers for amplification of the *PIK3CA* gene.

Primers	Forward	Reverse
exon9	GATTGGTTCTTTCCTGTCTCTG	CCACAAATATCAATTTACAACCATTG
exon20	TGGGGTAAAGGGAATCAAAAG	CCTATGCAATCGGTCTTTGC

Supplementary Methods

High-density genomic array analysis

DNA was prepared according to the manufacturer's instructions using the GeneChip mapping assay protocol for hybridization to GeneChip Mapping 50K Xba arrays (Affymetrix). Briefly, genomic DNA was digested with *Xba*I, ligated to an adaptor, and subjected to PCR amplification with adaptor-specific primers. The PCR products were digested with DNase I and labeled with a biotinylated nucleotide analog. The labeled DNA fragments were hybridized to the microarray and stained by streptavidin-phycoerythrin conjugates. SNP genotypes were assigned using the GTYPE 4.1 software (Affymetrix). Copy number analysis was performed using the CNAG 3.0 (Genome Laboratory, University of Tokyo, Tokyo, Japan). For data normalization, we used six normal reference samples. Genomic location of probes on the array was determined with the information in the University of California at Santa Cruz (UCSC) Genome Browser database. All raw data have been deposited in the Gene Expression Omnibus (GEO) database, www.ncbi.nlm.nih.gov/geo (accession no. GSE54509).

Gene expression analysis

Gene expression analysis was performed by a GeneChip system with a Human Genome U133 plus 2.0 array, which was spotted with 54,000 probe sets (Affymetrix) according to the manufacturer's instructions. Briefly, 200 ng of total RNA were reverse transcribed, amplified, and labeled using GeneChip 3’ IVT Express Kit (Affymetrix) following manufacturer’s instructions. The resultant labeled cRNA was then purified, fragmented, and hybridized to the Human Genome U133 plus 2.0 array at 45˚C for 16 h. The arrays were washed, stained with streptavidin-phycoerythrin, and scanned using a probe array scanner. The acquisition and initial quantification of array images were conducted using GeneChip Command Console Software (Affymetrix), then data were analysed by GeneSpring GX Software (Agilent Technologies). All raw data have been deposited in the GEO database, www.ncbi.nlm.nih.gov/geo (accession no. GSE43017).

Mutational analysis

Each coding exon of *PTEN* or *NDRG2* and *PIK3CA* exons 9 and 20 were amplified by PCR with 100 ng of genomic DNA and 0.5 μM specific primers from introns in a volume of 20 μl. Supplementary Tables 9, 10, and 11 show the sequences of primer sets for each exon of the three genes. PCR products were subjected to direct nucleotide sequencing. SNPs were selected from the National Center for Biotechnology Information (NCBI) database.

Infinium assay

High-molecular-weight DNA was prepared by phenol-chloroform extraction. Five-hundred-nanogram aliquots of DNA were subjected to bisulfite conversion using an EZ DNA Methylation-Gold™ Kit (Zymo Research). Subsequently, DNA methylation status at 27,578 CpG loci was examined at single-CpG resolution using the Infinium HumanMethylation27 Bead Array (Illumina). This array contains CpG sites located within the proximal promoter regions of the transcription start sites of 14,475 consensus coding sequences in the NCBI database. On average, two assays were selected per gene and from 3 to 20 CpG sites for more than 200 cancer-related and imprinted genes. Forty control probes were employed for each array; these included staining, hybridization, extension, bisulfite conversion, and negative controls. An Evo robot (Tecan, Switzerland) was used for automated sample processing. Whole-genome amplification was performed using the Infinium Assay Kit (Illumina)[1]. After hybridization, the specifically hybridized DNA was fluorescence-labeled by a single-base extension reaction and detected using a BeadScan reader (Illumina) in accordance with the manufacturer's protocols. The data were then assembled using GenomeStudio methylation software (Illumina). At each CpG site, the ratio of the fluorescent signal was measured using a methylated probe relative to the sum of the methylated and unmethylated probes, i.e., the so-called β-value, which ranges from 0.00 to 1.00, reflecting the methylation level of an individual CpG site.

Methylation-specific PCR (MSP)

Methylation-specific PCR was carried out using either a methylation-specific primer set (Methyl/NDRG2/forward 5'-TTTTTCGGGTATTGCATTTAGC-3', Methyl/NDRG2/reverse 5'-TAAATAAACAAACGCAAAAACGAA-3') or an

unmethylation-specific primer set (Unmethyl/NDRG2/forward 5'-TTTTTTGGGTATTGTATTTAGT-3' Unmethyl/NDRG2/reverse 5'-TAAATAAACAAACACAAAAACAAA-3') (nucleotides 20564128-20563929, GenBank accession no. NC_000014) at the following conditions: 98°C for 30 s; 40 cycles of 98°C for 10 s, 64°C (methylation) or 60°C (unmethylation) for 5 s, and 72°C for 30 s; and final extension at 72°C for 3 min. After agarose gel electrophoresis, the methylation status of the *NDRG2* promoter was classified as methylated, partially methylated, or unmethylated.

PI3K activity assay

The PI3K activity was measured using a PI3-Kinase Activity ELISA Assay kit (Echelon Biosciences) according to the manufacturer's instructions. Cells were lysed with lysis buffer (20 mM Tris-HCl pH 7.4, 137 mM NaCl, 1 mM $CaCl_2$, 1 mM $MgCl_2$, 1 mM sodium orthovanadate, 1% NP-40) supplemented with protease inhibitor cocktail (Sigma-Aldrich), and the cell lysates were subjected to immunoprecipitation with an anti-PI3K p85 antibody (1:200). The immunoprecipitated PI3K was incubated with the $PI(4,5)P_2$ substrate, and the generated $PI(3,4,5)P_3$ was assayed by competitive ELISA. The absorbance was read at 450 nm on a plate reader.

Supplementary Reference

1 Bibikova, M. *et al.* Genome-wide DNA methylation profiling using Infinium® assay. *Epigenomics* **1,** 177-200 (2009).